Journal of Medicinal Chemistry

Article

pubs.acs.org/jmc

A New Class of Antimalarial Dioxanes Obtained through a Simple Two-Step Synthetic Approach: Rational Design and Structure–Activity Relationship Studies

Marco Persico,[†,⊥,#] Arianna Quintavalla,[‡,⊥] Francesca Rondinelli,[†,⊥,#] Claudio Trombini,[‡] Marco Lombardo,*[,‡] Caterina Fattorusso,*[,†,#] Valeria Azzarito,[∥] Donatella Taramelli,[§,#] Silvia Parapini,[§,#] Yolanda Corbett,[§,#] Giuseppina Chianese,[†,#] Ernesto Fattorusso,[†,#] and Orazio Taglialatela-Scafati[†,#]

[†]Dipartimento di Chimica delle Sostanze Naturali, Università di Napoli "Federico II", Via D. Montesano, 49 I-80131 Napoli, Italy

[‡]Dipartimento di Chimica "Giacomo Ciamician", Alma Mater Studiorum, Università di Bologna, Via Selmi, 2 I-40126 Bologna, Italy

[§]Dipartimento di Sanità Pubblica, Microbiologia, Virologia, Università di Milano, Via Pascal 36, I-20133 Milano, Italy

[∥]School of Chemistry, University of Leeds, Woodhouse Lane, Leeds, LS29JT, U.K.

[#]Italian Malaria Network - Centro Interuniversitario di Ricerche sulla Malaria (CIRM), Dipartimento di Genetica, Biologia e Biochimica, Università di Torino, via Santena 19, I-10126 Torino, Italy

Supporting Information

ABSTRACT: A new series of simple endoperoxides, characterized by a 3-methoxy-1,2-dioxane scaffold, was designed on the basis of a previously developed pharmacophore. Through a simplified and versatile scheme of synthesis, which utilizes cheap and commercially available starting materials, it was possible to obtain several structurally and stereochemically different compounds that were tested against *P. falciparum*. Most of compounds showed antimalarial activity in the low micromolar range and no cellular toxicity, all being significantly more active on chloroquine resistant (CQ-R) than on chloroquine sensitive (CQ-S) strains. Resulting structure–activity relationships were analyzed by means of experimental and computational techniques, validating our design rationale and tailoring it for the new scaffold. Our study demonstrated that according to the hypothesized mechanism of action, the antimalarial activity can be improved through rational structural modifications, paving the way for the development of new simplified antimalarial endoperoxides.

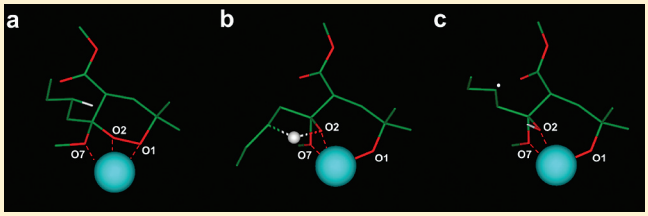

INTRODUCTION

Malaria infections continue to affect about 30% of world population and to cause 250–300 million clinical episodes per year, resulting in about one million deaths. Sub-Saharan Africa is the world region with the highest rate of infections, and children under 5 years of age play a dramatically high role in determining the death numbers.[1] The growth of the malarial burden experienced in recent years has been attributed to the increase in the population movements into malarial regions, to climate changes, and above all to the proliferation of multidrug resistant *Plasmodium falciparum* (*Pf*) parasites.[2] Indeed, the few low-cost drugs available (e.g., quinine, chloroquine) are those for which the parasites have developed resistance over the past several years, while more effective drugs, as artemisinin-based combinations, are still too expensive for the poorest people of malaria endemic regions. Moreover, the neurotoxicity associated with the use of artemisinins[3] and the reported cases of clinical resistance[4] to currently used artemisinin derivatives strongly encourage the finding, as soon as possible, of viable alternatives to the existing therapeutic options. In this regard, an intense international campaign has been launched by several public agencies aimed at the elimination and eventual eradication of malaria (Global Malaria Action Plan, http://www.rollbackmalaria.org/gmap/). The discovery of new and effective antimalarial agents will play a crucial role in the frame of a multifactorial strategy, including also prophylaxis, vaccines, and insecticides.

In the course of our ongoing search for antimalarial hits from marine sources, we have reported that plakortin (**1**) and its 9,10-dihydroderivative **2** (Chart 1), simple endoperoxide-containing polyketides isolated from the Caribbean sponge *Plakortis simplex*,[5] possess a significant in vitro antimalarial activity on CQ-R *Pf* strains and no cellular toxicity.[6]

Chart 1. Plakortin (1) and Dihydroplakortin (2)

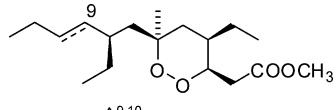

1 $\Delta^{9,10}$

2 9,10-dihydro

Received: August 5, 2011
Published: November 4, 2011

Scheme 1. Proposed Antimalarial Mechanism of Action of Plakortin (1) and Dihydroplakortin (2)

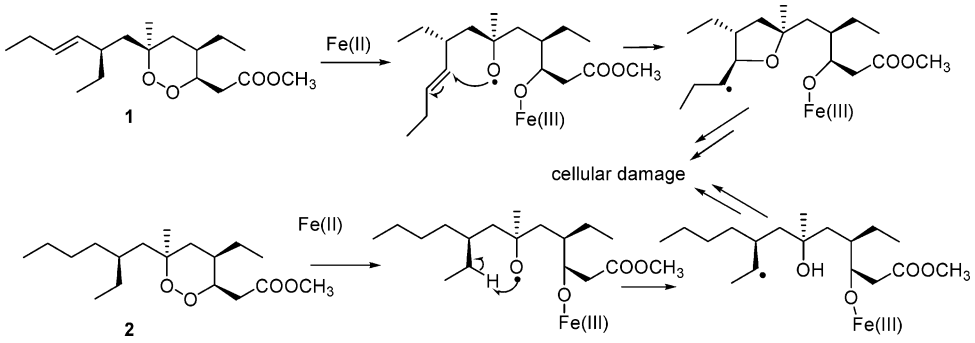

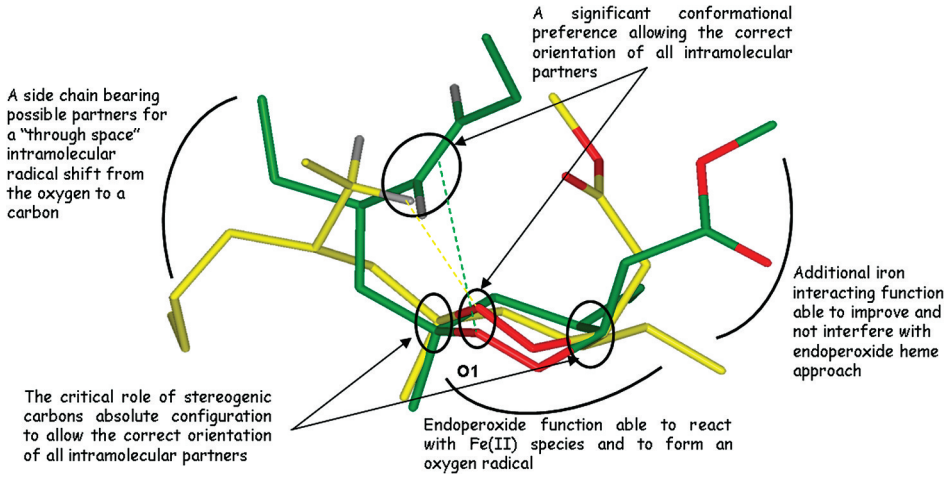

Figure 1. Plakortin (C atoms, green; O atoms, red) and dihydroplakortin (C atoms, yellow; O atoms, red) pharmacophores. Dotted lines highlight the radical shift occurring from O1 to the alkyl side chain. Hydrogen atoms with the exception of those bound to C_9–C_{10} (plakortin) and to C_{13} (dihydroplakortin) are omitted for clarity of presentation. Figure adapted and reproduced from ref 14. *Org. Biomol. Chem.* **2010**, *8*, 846–856 (http://dx.doi.org/10.1039/b918600j). Reproduced by permission of The Royal Society of Chemistry.

A multidisciplinary approach (including computational and experimental studies) on natural analogues[7,8] and semisynthetic derivatives[9] provided some valuable insights about the SARs needed for the antimalarial activity of these simple 1,2-dioxanes. These results unambiguously indicated the crucial role of the endoperoxide functionality, suggested the importance of the "Western" alkyl side chain, and revealed conformation-dependent features critical for antimalarial activity.[9]

The mechanism of action of artemisinin, the parent compound of endoperoxide antimalarials, is still the object of an intense debate;[10,11] however, there is a general agreement on the fact that this molecule, after in situ activation, acts by perturbing the redox balance within the "sensible" parasite cell.[12,13] In a recently reported investigation based on a combined chemical and computational approach,[14] we proposed that molecules belonging to the plakortin family, upon interaction with Fe(II), undergo a dissociative electron transfer (DET) of the endoperoxide bond, giving rise to an oxygen-centered radical. A fast "through space" 1,4- (**1**) or 1,5- (**2**) intramolecular radical shift to a Western side chain carbon atom occurs through a radical cascade that leads to the putative toxic species for the Plasmodium environment (Scheme 1). In this scenario, several studies indicated that heme, abundantly produced within the parasite food vacuole as a result of hemoglobin digestion, represents the main molecular target of antimalarial endoperoxides.[11,15]

Indirect support of this mechanism comes from the inactivity of those plakortin analogues, which experience steric problems when reactive iron species approach the endoperoxide oxygens (as manadoperoxides),[16] as well as from the very low activity of those plakortin analogues for which the orientation of reaction partners does not allow any intramolecular radical shift.[9,17]

The acquired information suggested that the essential pharmacophoric requirements for antimalarial activity should include (i) a 1,2 dioxane ring able to react with Fe(II) species through its endoperoxide group, forming an oxygen radical, (ii) a side chain bearing possible partners for a "through-space" intramolecular radical shift to a carbon atom, (iii) configurational and conformational features that allow accessibility of iron to 1,2-dioxane oxygens as well as the correct orientation of all the intramolecular reaction partners, (iv) iron interacting with additional functionalities, favoring the approach to heme without interfering with the redox reaction, and (v) the ability of the generated carbon radical to propagate via intermolecular reactions (Figure 1).

We believe that the information now available for plakortin antimalarials could be fruitfully used to design a new chemotype of antimalarial agents based on the simple, monocyclic 1,2-dioxane scaffold. Ideally, this simplified structure could allow an efficient chemical synthesis amenable to large-scale preparation of new antimalarials at low cost. As suggested by the target product profile (TPP) published by Medicine for Malaria Venture (MMV) in September 2010, cheapness is a crucial requirement for antimalarial drugs of the next generation. According to MMV, a likely clinical candidate

Scheme 2. Manganese(III) Acetate Promoted Synthesis of 1,2-Dioxane-3-ols 5

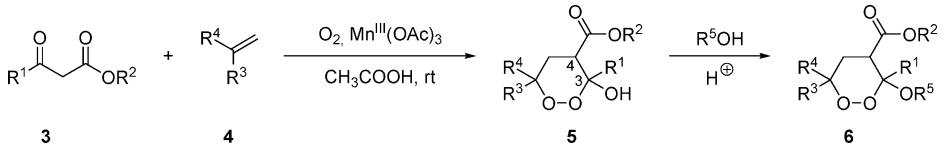

should have oral activity with SERC (single exposure radical cure) and a cost treatment of less than $1 for uncomplicated malaria.[18] Moreover, the simplification of the molecular scaffold compared to artemisinin could reduce the incidence of neurotoxic effects like those reported for some oil soluble artemisinin derivatives.[3]

Taking into account the developed pharmacophore model (Figure 1), we herein disclose the design, the synthesis, the biological evaluation, and the 3D-SAR studies for a novel series of 1,2-dioxane antimalarials obtained by means of an efficient one-pot three-component Mn(III)-mediated synthesis that utilizes cheap starting materials. The obtained molecules are 3,6,6-trialkyl-3-methoxy-1,2-dioxanes with simple alkyl chains and bearing an ester group at position 4. Through our simplified and versatile scheme of synthesis it was possible to obtain several structurally and stereochemically different compounds that were tested against *Pf*. The results allowed us to validate our design rationale and tailor it for the new scaffold. Therefore, by use of the same synthetic approach, the acquired information will allow the preparation of new optimized antimalarials.

RESULTS AND DISCUSSION

Chemistry. In the past few decades, a large number of synthetic endoperoxides (1,2-dioxolanes and 1,2-dioxanes),[17,19,20] 1,2,4-trioxolanes,[21] 1,2,4-trioxanes,[22,23] and 1,2,4,5-tetraoxanes[24,25] have been synthetized and studied as potential antimalarial drugs for treatment of CQ-R *Pf* infections. The current status of synthetic peroxides inspired by artemisinin and other naturally occurring peroxides has been examined in recent review articles.[26−28]

In 1990, Nishino and co-workers reported a seminal research work on the synthesis of 1,2-dioxane-3-ol scaffolds (**5**) by the manganese(III) acetate promoted formal [2 + 2 + 2] cycloaddition of activated methylene compounds (i.e., *β*-ketoesters **3**), olefins (**4**), and molecular oxygen (Scheme 2),[29] a reaction first reported in 1989 to proceed under electrochemical oxidation conditions or by AIBN-promoted radical cascade.[30] The formal catalytic cycle is based on the key generation of enol radicals **A** by oxidation of **3** using Mn(III) acetate, as depicted in Scheme 3.[31]

In terms of structural versatility and flexibility, 1,2-dioxane **5** exhibits three interesting features: (i) substituents R^1-R^4 can be varied as a result of a rational choice of the *β*-ketoester **3** and the alkene component **4**; (ii) the ester attached at C-4 offers manifold opportunities for chemical transformations (reductions, amide formation, etc.); (iii) the hemiketal group on C-3 can be converted into the corresponding ketal **6** upon incorporation of a suitable alcohol (R^5OH, Scheme 2). Reactions are carried out in glacial acetic acid at room temperature. Manganese(III) acetate initially was insoluble in acetic acid at room temperature, but in the presence of an activated methylene compound, it gradually dissolves, suggesting the formation of a new Mn(III) complex by ligand exchange. The in situ generated Mn(III) enolate rapidly collapses into the electrophilic carbon radicals **A** by single electron transfer from the electron-rich carbon−carbon double

Scheme 3. Formal Catalytic Cycle for the Mn(III) Acetate Promoted Synthesis of 1,2-Dioxane-3-ols 5

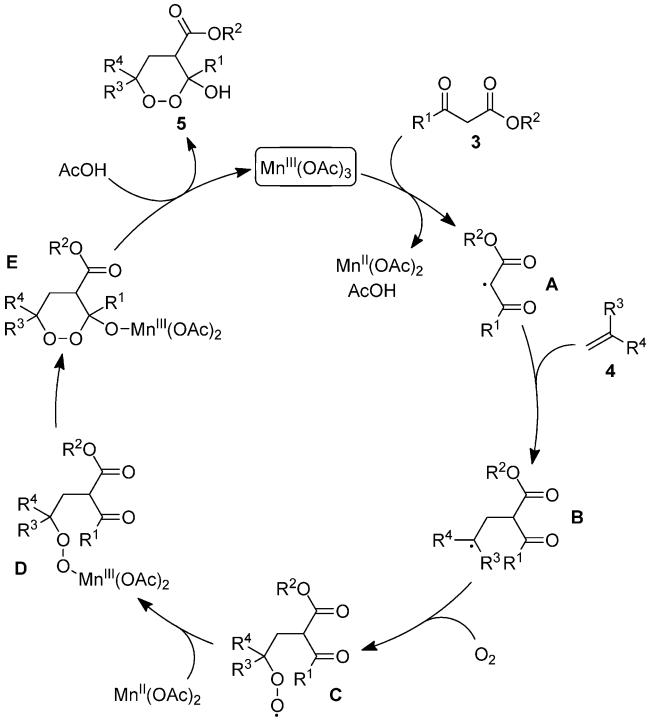

bond to Mn(III).[32] When the reaction is carried out at room temperature in the presence of an olefin (typically a *gem*-disubstituted alkene) and molecular oxygen, **A** adds first to the alkene, providing the nucleophilic carbon centered radical **B**, which then takes up oxygen dissolved in acetic acid to produce **C**. A new one-electron transfer from Mn(II) to **C** restores Mn(III) and generates the hydroperoxy anion **D**, which rapidly collapses to **E** by ring−chain tautomerism. Acidic quenching by acetic acid affords the target 1,2-dioxane-3-ol **5**, restoring Mn(III) acetate in solution. The electronic properties of the intermediate free-radicals determine the order of the radical cascade and reduce the side reactions such as the homocouplings of **A** and **C**, as well as the combination of molecular oxygen, an electrophilic biradical, with the electrophilic enol radical **A**. This catalytic process has been reported to work efficiently with 1,1-diarylethenes, affording remarkable yields of the expected cycloadducts. Considerably lower are the conversions reported with *gem*-disubstituted aliphatic alkenes. In principle, with this family of alkenes, off-cycle redox reactions can have a significant impact on the final yields in 1,2-dioxane-3-ol **5**. For example, free radical **B** may be overoxidized by Mn(III) to a carbenium ion that stabilizes upon cyclization to dihydrofuran **7** (Scheme 4). Finally, alkene itself may be oxidized by Mn(III) in acetic acid, thus contributing to the presence of side products together with homocoupling reactions.

After several optimization runs, the best experimental conditions in terms of yields and purity of the products were

dx.doi.org/10.1021/jm201056j | J. Med. Chem. 2011, 54, 8526−8540

Scheme 4. Manganese(III) Acetate Promoted Overoxidation of Carbon Radical B to Dihydrofuran 7

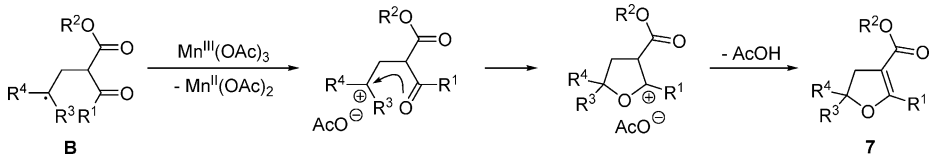

reached by using (i) a catalytic amount of Mn(III) acetate (10 mol %), (ii) a stoichiometric amount of Mn(II) acetate, (iii) a 3:1 molar ratio between the β-ketoester **3** and the alkene **4**, and (iv) oxygen at atmospheric pressure with acetic acid as solvent at room temperature. In all cases, the examined products were obtained in fair to good isolated chemical yields (39−89%). In the case of symmetrically disubstituted ($R^3 = R^4$) alkenes **4**, a single diasteroisomer of the product **5** was identified in the crude reaction mixture and isolated by flash chromatography, possessing the hydroxyl group at C-3 and the carbomethoxy at C-4 in a cis stereorelationship and adopting a preferred conformation with the hydroxyl group in the axial position. This was determined through complete assignment of ^{1}H NMR resonances followed by interpretation of cross-peaks in the 2D NMR ROESY spectrum (correlations H-4/alkyl group at C-6; H-4/alkyl group at C-3) (Figure 2). On the other hand, when nonsymmetrically

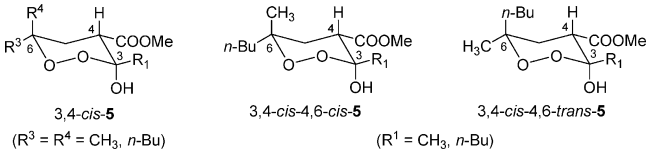

Figure 2. Most stable conformers of the products isolated from Mn(III) acetate promoted cycloaddition.

disubstituted alkenes were used, only two of the four possible diastereoisomers were obtained and isolated, again possessing a fixed 3,4-cis stereorelationship but differing in the configuration at C-6 (Figure 2). The preferential formation of 3,4-cis stereoisomers was already noticed by Nishino,[29−31] and it is likely the consequence of a stereospecific attack of the hydroperoxy oxygen at the ketone group, determined by the configuration at C-4.

All the intermediate 1,2-dioxane-3-ols were tested for their in vitro antimalarial activity against both CQ-S (D10) and CQ-R (W2) *Pf* strains, and all were completely inactive (IC_{50} > 30 μM). This result was not surprising, since a very low antimalarial activity has already been reported for other hemiketal endoperoxides.[33] Thus, the 1,2-dioxane-3-ols were transformed into the corresponding methyl ketal derivatives **8**−**14**. The ketalization reaction proved to be less easy than hoped, and after screening several different reaction conditions, we found the best results in terms of yields by using camphorsulfonic acid (CSA) as the promoter in the presence of methyl orthoformate at room temperature for 72 h.

According to this procedure, 1,2-dioxanes **8**−**14** were prepared (Figure 3) that show different permutations of R^1, R^3, and R^4 substituents, corresponding mainly, but not exclusively, to methyl or *n*-butyl groups.

When the reagent mixture consisted of a single diastereomer (see Table 1), two diasteromeric products were isolated, derived from a partial epimerization at C-3 during the ketalization process, with diastereoselecivities in the 50:50 to 70:30 range in favor of the 3,4-cis adduct. When a mixture of

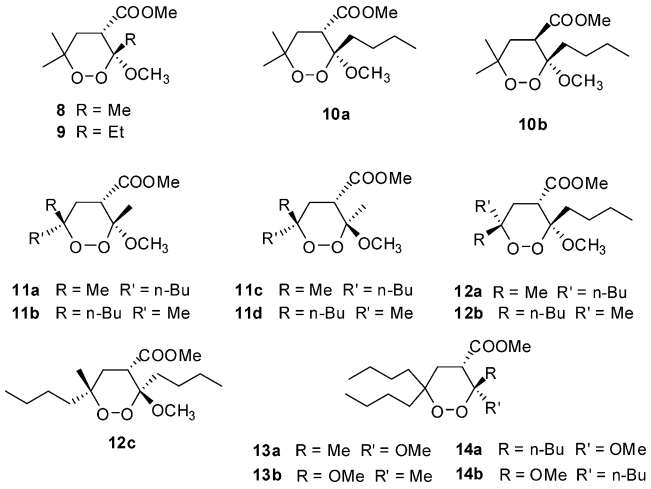

Figure 3. (±)-1,2-Dioxanes **8**−**14**.

two diasteromeric 1,2-dioxane-3-ols **5** was used (see Table 1), a more complex mixture of diasteromers was isolated but the same stereochemical trend was observed. Table 1 summarizes conditions and results of the synthesis of methyl ketals **8**−**14**. Of course, all the compounds shown in Figure 3 and reported in Table 1 have been obtained as racemic mixtures. All the diastereomeric mixtures were separated by gravity column chromatography followed by direct phase HPLC. Then complete NMR assignments were obtained on the isolated diastereomers through 2D NMR spectroscopy (COSY, HSQC, HMBC experiments). Finally, the relative configuration around the six-membered ring was determined for each compound through inspection of the 2D NMR ROESY experiments. For example, the ROESY cross-peaks of H-4 (δ 3.07) with H_2-1″ z(δ 1.83 and 1.70) and of H-5ax (δ 2.23) with Me-6 (δ 1.16) and with OMe-3 (δ 3.31) were used to infer the relative configuration of compound **12b** (Figure 4).

To overcome the partial isomerization at C3 in the acid-catalyzed ketalization step, we attempted a different approach to **6**, treating **5** with a strong base in THF in the presence of an excess of CH_3I. Surprisingly, under these conditions no trace of methyl ketals was detected; however, methylation at C4 did occur.

In Vitro Antimalarial Activity. The 1,2-dioxane-3-*O*-methyl derivatives **8**−**14** have been tested for their in vitro antimalarial activity against both CQ-S (D10) and CQ-R (W2) *Pf* strains. Results summarized in Table 2 show that most of these compounds have antimalarial activity in the low micromolar range. In addition, all the compounds showed activity against the CQ-R strain higher than against the CQ-S strain.

When tested for cellular cytotoxicity against a human endothelial cell line, human microvascular endothelial cell line (HMEC-1), compounds **10a**, **12b**, **13b**, and **14a** were not toxic (Table 3) with a therapeutic index ranging from 90 to 250 (calculated on CQ-R strains). Calculated log *D* for the newly

dx.doi.org/10.1021/jm201056j | J. Med. Chem. 2011, 54, 8526−8540

Table 1. Synthesis of Methyl Ketals 8−14[a]

substituent	compd **5**, yield (%)	diastereomeric ratio of **5**	methyl ketals **8−14**, yield (%)	diastereomeric ratio of **8−14** (3,4 cis/trans)
$R^1 = R^3 = R^4 = CH_3$	89	3,4-cis (100%)	**8** (81%)	70:30
$R^1 = Et\ R^3 = R^4 = CH_3$	39	3,4-cis (100%)	**9** (48%)	70:30
$R^1 = Bu\ R^3 = R^4 = CH_3$	65	3,4-cis (100%)	**10a,b** (69%)	70:30
$R^1 = R^3 = CH_3\ R^4 = Bu$	54	3,4-cis/4,6-cis (50%)	**11a−c** (40%)	60:40
		3,4-cis/4,6-trans (50%)	**11b−d** (40%)	60:40
$R^1 = R^3 = Bu\ R^4 = CH_3$	64	3,4-cis/4,6-cis (50%)	**12a−c** (30%)	60:40
		3,4-cis/4,6-trans (50%)	**12b** (30%)	>95:5[b]
$R^1 = CH_3\ R^3 = R^4 = Bu$	71	3,4-cis (100%)	**13a,b** (73%)	60:40
$R^1 = R^3 = R^4 = Bu$	53	3,4-cis (100%)	**14a,b** (44%)	50:50

[a]Conditions: CSA (5.0 equiv), methyl orthoformate (2 equiv), MeOH (0.14 M), room temp for 72 h. [b]The minor 3,4-trans/4,6-trans stereoisomer was not detected or isolated.

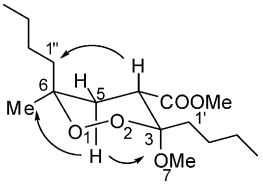

Figure 4. Determination of relative configuration for compound **12b** through ROESY correlations.

synthesized endoperoxides ranges from 1.62 to 6.04, while the molecular weight varies from 218.25 to 344.49 Da (Table 1SI). In general, log *D* between 0 and 5 and a molecular weight of <500 Da constitute optimal physical properties for passive drug absorption. These results, although incomplete, suggest that this class of compounds is suitable for further development.

Reaction with Fe(II) Chloride. The exact molecular mechanism underlying the biological activity of artemisinin and that of related antimalarial endoperoxides is still a matter of debate.[10] The interaction with Fe(II) heme and the consequent oxidative stress in the plasmodium are believed to play a major role in this bioactivity.[11,12] It has been proposed[34] that the reaction of endoperoxides with Fe(II) involves a one-electron reduction leading to the cleavage of the oxygen−oxygen bond with the consequent formation of an oxygen anion bound to iron and of an oxygen free radical. Two possible evolutions of the generated oxygen radical have been postulated for artemisinin (Scheme 5), principally on the basis of theoretical studies[35] and of model reactions in vitro with heme or with Fe(II) inorganic salts,[36] which were used to mimic the antimalarial mechanism of action. In pathway 1, the oxygen O1 radical evolves through an intramolecular 1,5-H shift leading to a secondary carbon radical, while alternatively in pathway 2, the oxygen O2 radical evolves through a homolytic carbon−carbon cleavage of the C3−C4 bond.

Assuming that reaction with Fe(II) inorganic salts could give interesting information also in the case of the methyl ketal endoperoxides **8−14**, we selected three of them (**9**, **10b**, and **12b**), on the basis of the diversity of their structural and bioactivity features, as test compounds to carry out the reaction. Thus, compound **12b** was allowed to react with $FeCl_2$ (5 equiv) in CH_3CN/H_2O, 4:1, at room temperature for 2 h, and chromatographic purification of the reaction mixture afforded as major products unreacted **12b** and the lactone **15** (Scheme 6), whose stereostructure has been identified by detailed spectroscopic investigation. When compounds **9** and **10b** were allowed to react with $FeCl_2$ in the same conditions, both of them efficiently produced the same lactone **16** (Scheme 6).

The formation of compounds **15** and **16** can be rationalized through the mechanism shown in Scheme 7. Upon interaction with Fe(II) ion, the endoperoxide bond would be cleaved with regioselective formation of the oxygen radical at O2. Through the expulsion of a butyl (or ethyl) radical, this unstable intermediate would give rise to the methyl ester, which would then collapse into the final lactone.

The results of in vitro reaction of **9**, **10b**, and **12b** with $FeCl_2$ would indicate the carbon−carbon cleavage pathway as responsible for bioactivity. This is in perfect agreement with results described by Kobayashi and co-workers[37] for peroxyplakortic derivatives, natural methyl ketal endoperoxides bearing some structural relationships with compounds **8−14**. Following Scheme 7, the in vitro activity of these compounds should be ascribed to the toxic action on the parasite environment exhibited by the alkyl radicals released by means of the homolytic carbon−carbon cleavage. However, this mechanistic hypothesis does not agree with results obtained for compounds **9**, **10b**, and **12b**. Indeed, the fact that the active (e.g., **12b**, Table 2) and inactive (e.g., **9** and **10b**, Table 2) compounds gave, with similar efficiency, the same primary carbon (**10b** and **12b**) or strictly related (**9**) one is unambiguous evidence of the lack of any direct correlation between the observed carbon−carbon cleavage reactions and the antimalarial activity.

These results are in agreement with structure−activity relationship (SAR) studies reported for artemisinins[12,36a,38] as well as for other endoperoxide derivatives,[37] failing to relate the favored in vitro carbon−carbon cleavage pathway with antimalarial activity, which is instead related to the intramolecular H-shift mechanism. Thus, in the 3-methoxy-1,2-dioxanes **8−14**, where both mechanisms (H-shift and carbon−carbon cleavage) can operate, the model reaction with $FeCl_2$ does not meet with the in vivo outcome of the reaction. In this scenario, a separate case is represented by non-ketal monocyclic endoperoxides, as plakortins, where the carbon−carbon cleavage mechanism does not occur[14] (see Scheme 1) likely because of the lack of the driving force conferred by the formation of the stable ester group[39] (see Scheme 7). Indeed, the reaction of plakortins with $FeCl_2$ indicated exclusively the "through space" intramolecular shift of the oxygen radical,[14] accounting for the observed SARs of plakortins and related non-ketal monocyclic endoperoxides.[9,16,17]

As we will discuss in the next paragraph, also in the case of **8−14**, an intramolecular radical shift mechanism can well explain the marked difference of activity exhibited by very similar compounds (e.g., **9** and **10a**) or even by diastereoisomers (e.g., **10a** and **10b**), giving an overall rationale for all the SARs of this series of compounds.

Table 2. Antimalarial Activity of Methyl Ketals 8-14 against Chloroquine-Sensitive (D10) and Chloroquine-Resistant (W2) *P. falciparum* Strains

Compound	Structure	D10 IC_{50} (μM)[a]	W2 IC_{50} (μM)[a]
8	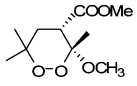	> 30	> 30
9	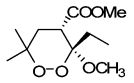	> 30	> 30
10a	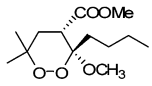	3.7 ± 0.2	1.5 ± 0.5
10b	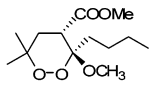	> 30	> 30
11a	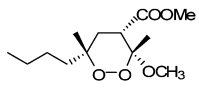	8.5 ± 3.8	4.9 ± 1.7
11b	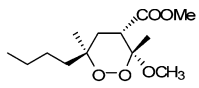	12.6 ± 6.0	11.8 ± 2.2
11c	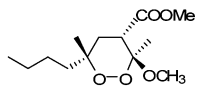	17.7 ± 4.0	8.4 ± 2.9
11d	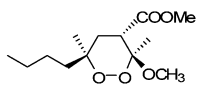	17.7 ± 2.9	6.4 ± 1.4
12a	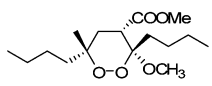	4.2 ± 1.0	1.5 ± 0.4
12b	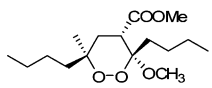	2.6 ± 0.2	1.3 ± 0.2
12c	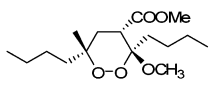	12.3 ± 1.7	5.0 ± 1.1
13a	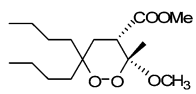	7.4 ± 1.1	2.5 ± 0.7
13b	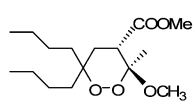	2.6 ± 0.7	0.8 ± 0.3
14a	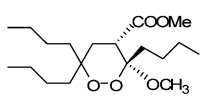	2.9 ± 0.6	1.2 ± 0.2
14b	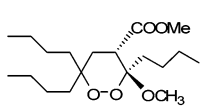	2.3 ± 0.6	1.2 ± 0.3
Chloroquine		0.029 ± 0.012	0.52 ± 0.02
1[b]		0.9 ± 0.4	0.4 ± 0.1

[a]Data are the mean ± SD of three different experiments in duplicate. [b]Data from ref 14.

Table 3. Cytotoxicity on Human Microvascular Endothelial Cell Line HMEC-1

compd	IC_{50} (μM)[a]
10a	>384
12b	167.3 ± 24.7
13b	98.3 ± 4.1
14a	107.9 ± 10.8

[a]Data are the mean ± SD of three different experiments in duplicate.

Scheme 5. Representation of the Artemisinin Postulated Mechanism of Action

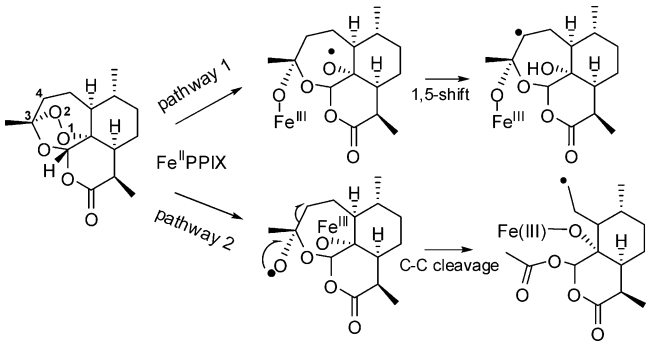

Scheme 6. Reaction of Compounds 12b, 9, and 10b with $FeCl_2$

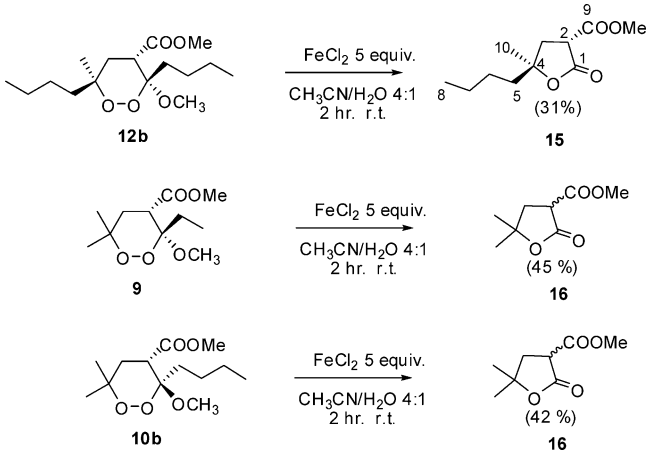

Scheme 7. Mechanism Postulated for the Formation of Compounds 15 and 16

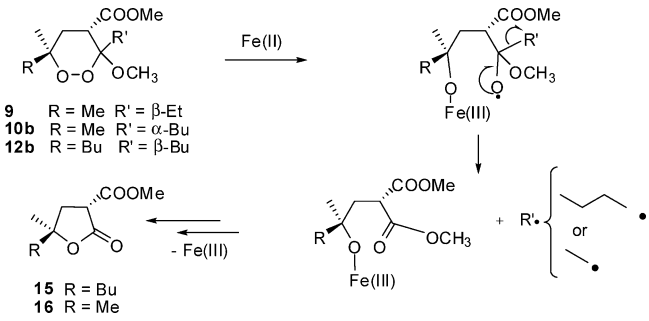

Structure–Activity Relationship Studies. An extensive molecular modeling study, including molecular mechanics (MM), dynamics (MD), and density functional theory (DFT) calculations, was undertaken to analyze **8–14** structure–activity relationships (SARs) (see Experimental Section for details). The above-reported series of derivatives, characterized by a 3-methoxy-1,2-dioxane scaffold (Table 2), was specifically

dx.doi.org/10.1021/jm201056j | J. Med. Chem. 2011, 54, 8526–8540

Table 4. Occurrence Rate (%) of 1,2-Dioxane Ring Conformations of 8−14 Considering PM6 Conformers within 5 kcal/mol from the Global Minimum

Cmp	Chair A	Chair B	Skew Boat A	Skew Boat B
8	48	13	26	13
9	43	13	34	10
10a	60	6	30	4
10b	49	17	29	5
11a	54	4	38	3
11b	58	4	35	2
11c	61	9	23	7
11d	52	16	25	7
12a	72	2	21	5
12b	62	4	28	6
12c	77	4	17	2
13a	67	5	26	2
13b	53	15	30	2
14a	71	2	25	2
14b	66	6	24	4

designed in order to investigate the antimalarial mechanism of action. This, indeed, represents a crucial issue for the development of new simplified antimalarial endoperoxides.

As discussed above, results obtained for compounds **9**, **10b**, and **12b** indicated that the antimalarial activity does not relate with the carbon−carbon cleavage observed in vitro upon their reaction with $FeCl_2$ (Schemes 6 and 7). Therefore, the newly designed compounds were subjected to an in-depth computational analysis, taking into account the "through space" radical shift mechanism already reported for plakortins[14] (Scheme 1). A simulated annealing procedure followed by molecular mechanics (MM) energy minimization and semiempirical PM6 full geometry optimization was applied. Low energy conformers (within 5 kcal/mol from the global minimum) were then classified and filtered on the basis of their (i) 1,2-dioxane ring conformation, (ii) distance of endoperoxide oxygens from a putative partner for a 1,5- or 1,4-intramolecular radical shift, and (iii) steric accessibility of endoperoxide oxygen lone pairs (Tables 4 and 5). The lowest energy conformers of each compound meeting the assumed pharmacophoric requirements were subjected to dynamic docking studies, with the compound in complex with heme. The resulting structures, again checked for their pharmacophoric features, represented putative bioactive conformations and were then subjected to DFT calculations.

First, a structural analysis revealed that the electronic repulsion between the ester carbonyl oxygen and the endoperoxide oxygen O2 (for atom numbering see Figure 4) and the steric repulsion between C-3 and C-4 substituents drive the conformational preference of the 1,2-dioxane ring. Consequently, in agreement with NMR data, all compounds showed a definite conformational preference for one ring chair conformation, named chair A, characterized by the equatorial position of the ester substituent at C-4 (Table 4). On the other hand, the steric repulsion between C-3 and C-6 substituents (Figure 5a) strongly reduced the rate of low energy conformers,

Table 5. Occurrence Rate (%) of PM6 Conformers within 5 kcal/mol from the Global Minimum with Interatomic Distances Suitable for a Radical Shift from O1 or O2 (≤ 3 Å) and Steric Accessibility of the Endoperoxide Oxygens Lone Pairs

	C3 axial alkyl side chain		C3 equatorial alkyl side chain		C6 axial alkyl side chain		C6 equatorial alkyl side chain	
compd[a]	1,4-H shift	1,5-H shift	1,4-H shift	1,5-H shift	1,4-H shift	1,5-H shift	1,4-H shift	1,5-H shift
8	0	0	0	0	0	0	0	0
9	0	0	32	0	0	0	0	0
10a	0	0	24[b]	3[b]	0	0	0	0
10b	17	1	0	0	0	0	0	0
11a	0	0	0	0	0	0	18[b]	6[b]
11b	0	0	0	0	21[b]	3[b]	0	0
11c	0	0	0	0	0	0	22[b]	3[b]
11d	0	0	0	0	20[b]	3[b]	0	0
12a	0	0	30[b]	2[b]	0	0	20	5
12b	0	0	23[b]	5[b]	20	1	0	0
12c	30	0	0	0	0	0	22[b]	4[b]
13a	0	0	0	0	14[b]	3[b]	16[b]	4[b]
13b	0	0	0	0	22[b]	1[b]	20[b]	4[b]
14a	0	0	13[b]	4[b]	9	0	16	2
14b	17	1	0	0	11[b]	0	18[b]	4[b]

[a]All compounds present chair A 1,2-dioxane ring conformations. [b]Putative bioactive conformations.

dx.doi.org/10.1021/jm201056j | J. Med. Chem. 2011, 54, 8526–8540

presenting intramolecular distances suitable for the 1,5-H shift (Table 5).

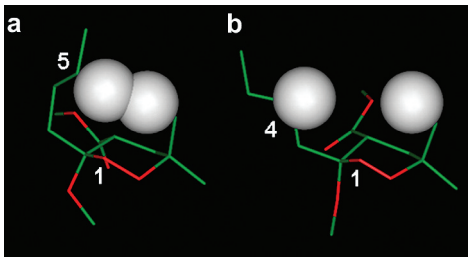

Figure 5. PM6 conformers of **10a** presenting intramolecular distances suitable for the 1,5-H shift (a) and 1,4-H shift (b). Atom numbering refers to the distance between H-shift possible partners. van der Waals volumes of the hydrogens responsible for steric hindrance between C3 and C6 substituents (a) are shown. Atoms are colored by atom type (C = green; O = red; H = white).

All the analyzed compounds presented a significant rate of low energy conformers able to undergo a 1,4-H shift from C3 and/or C6 alkyl chains to the oxygen radical (Table 5 and Figure 5b). The only exception is represented by compound **8**, which possesses only methyl substituents at C3 and C6, while compound **9** could undergo a 1,4-H shift but only forming a primary carbon radical.

In order to evaluate the possible role of solvent for the molecular conformations of the new simplified 1,2-dioxanes, MD, MM, and DFT calculations including the implicit solvent were also performed, and the obtained results indicated that the conformational behavior is not affected (Table 2SI, Figure 1SI).

The reliability of our DFT study in calculating the chemical physical parameters of the endoperoxide bond has been assessed through the analysis of vibrational frequencies associated with O1−O2 stretching. According to our results the O1−O2 stretching band, combined with other vibrational modes, should occur at a wavelength between 750 and 911 cm^{-1}, with the frequency band at 894 and 911 cm^{-1} exhibiting the strongest O1−O2 stretching character (Table 3SI, Figure 2SI). Our DFT data are in agreement with previously reported theoretical data indicating that the two characteristic bands at 831 cm^{-1} and 723 cm^{-1} observed in the experimental studies on artemisinin are scarcely related to motions of the peroxide linkage.[40] The related O1−O2 bond distance of 1.454 Å is in agreement with the experimental determined value of the endoperoxide bond length.[40c]

The results of DFT calculations indicated that in the absence of iron there is no definite preference between O1 and O2 for the acquisition of the radical after the O−O reductive scission, as demonstrated by the analysis of atomic polar tensor (APT) charges and Mulliken and natural bond order (NBO) spin densities on O1 and O2 (Table 4SI, Figure 3SI). Thus, iron coordination and possible radical evolution are supposed to be determinant for the formation of the radical on one oxygen rather than the other. To investigate this issue, the putative bioactive conformations, obtained by MM and MD calculations, in complex with Fe(II) were optimized at density functional level of theory. All possible iron coordination complexes were generated (hereafter named O1/O2, O1/O7, O2/O7, O1/O2/O7 according to the iron interacting oxygens, O7 being the methoxy group at C3) and were then used as starting structures for the DFT study. It is emphasized that O1/O7 and O1/O2/O7 complexes are only possible when the methoxy group at C3 is in the axial position, as it occurs in compounds **10a**, **11a**,**b**, **12a**,**b**, **13a**, and **14a**. In this case, the O1/O7 and the O2/O7 starting complexes always converged to the more energetically favored O1/O2/O7 complex while the O1/O2 starting complex led to a O2−C3 scission product (Figure 6a,b).

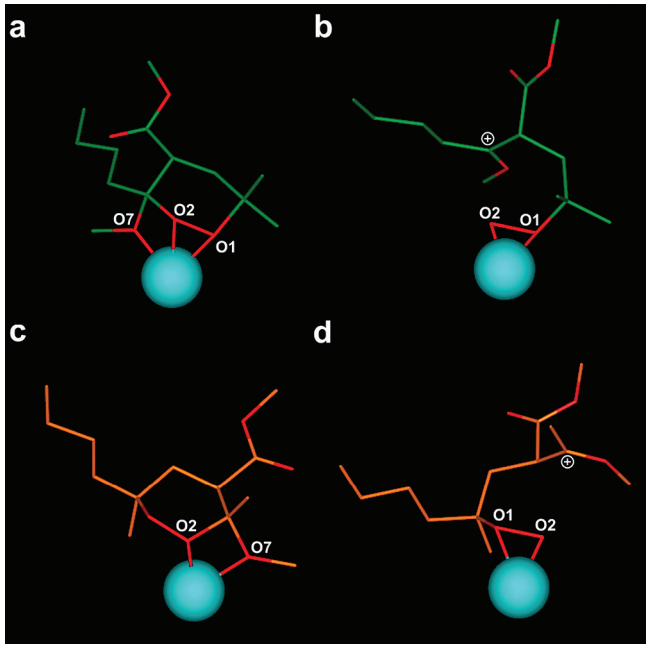

Figure 6. DFT structures of **10a** and **11c** bioactive conformers in complex with Fe(II): (a) **10a** O1/O2/O7 complex; (b) **10a** scission product of the O1/O2 complex; (c) **11c** O2/O7 complex; (d) **11c** scission product of the O1/O2 complex. van der Waals volume of iron is shown (scaled by 50% for clarity of presentation). The oxygens interacting with iron are labeled. Atoms are colored as follows: C = green (**10a**); orange (**11c**); O = red; Fe(II) = cyan. Hydrogens are omitted for sake of clarity.

The calculated ΔE between the low energy iron tricoordinated complex (Figure 6a) and the heterolytic scission product obtained by O1/O2 iron coordination (Figure 6b) is quite low (~3 kcal/mol). This latter resulted from the Fe(II) induced cleavage of the ketal to form a cation at C3 which is stabilized by mesomeric effect of the methoxy group and by the spatial proximity of the ester carbonyl oxygen (2.6 Å). A comparable oxygen−carbon heterolytic scission product has been proposed to be responsible for the antimalarial activity of artemisinin.[41] Nevertheless, it has been argued[12] that the oxygen−carbon heterolytic cleavage mechanism does not account for the reported different antimalarial activities of artemisinin derivatives able to form virtually the same carbocation.[42] Analogously, there is no relation between the antimalarial acitivity of derivatives **8**−**14** (Table 2) and the formation of a carbocation at C3 (e.g., **8** vs **10a**, Table 2). Thus, it is likely that the O2−C3 heterolytic scission, promoted by O1/O2 iron coordination, competes with the mechanism responsible for the antimalarial activity subtracting some bioactive compound. Results obtained on the prereactive complex indicated that only O1/O2/O7 iron coordination can give rise to the 1,4-H shift generating the putative toxic carbon radical. The calculations performed on the putative carbon radical intermediate, in complex with Fe(III), confirmed these data. In fact, in the case of compound **10a**, only starting from the O1/O2/O7 complex made it possible to

dx.doi.org/10.1021/jm201056j | J. Med. Chem. 2011, 54, 8526–8540

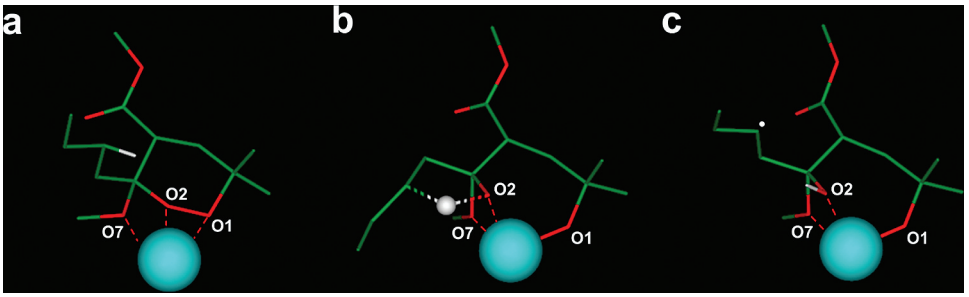

Figure 7. 10a prereactive complex (a), transition state (b), and carbon radical intermediate (c). Metal bonds are depicted as solid lines for anionic oxygen O1 and as dashed lines for O2 and O7. The carbon radical is indicated by a white dot. van der Waals volume of iron is shown (scaled by 50% for clarity of presentation). Hydrogens are omitted for the sake of clarity with the exception of that involved in the 1,4-H shift, depicted in stick (a and c) or in ball (b). Atoms are colored as follows: C = green; O = red; H = white; Fe(II) = cyan.

obtain a stable carbon radical intermediate, which corresponded to the hypothesized 1,4-H shift between C3 butyl chain and O2 (Figure 7c).

In agreement with the calculated distance in the O1/O2/O7 prereactive complex (Figure 7a; Fe(II)−O1 = 1.96 Å, Fe(II)−O2 = 2.25 Å, Fe(II)−O7 = 1.96 Å), the transition state (TS) complex of **10a** presented O1 interacting with Fe(III) as an anion and O2 reacting with the alkyl chain as a radical (Figure 7b; Fe(III)−O1 = 1.76 Å, Fe(III)−O2 = 1.99 Å, Fe(III)−O7 = 1.99 Å). This result indicates that after the reductive scission of the endoperoxide bond, when the methoxy group is in the axial position, the radical is preferentially formed on the oxygen that is more distant from Fe(II) in the prereactive complex (i.e., O2) (Figure 7b).

On the other hand, compounds presenting the methoxy substituent in the equatorial position, such as **10b**, **11c,d**, **12c**, **13b**, and **14b**, resulted in coordinating Fe(II) only by O2 and O7 (Figure 6c) because of the fact that O1/O2 starting complex led to the same O2−C3 scission product observed for compounds with axial methoxy group (Figure 6d). As a consequence, contrary to what happened for **10a** (axial methoxy group), compound **10b** (equatorial methoxy group) is not able to give rise to O1/O2/O7 coordination while O2/O7 chelation could occur. Nevertheless, because of the overlapping of the van der Waals volumes of iron and the C3 alkyl chain hydrogen involved in the putative 1,4-H shift (Figure 4SI), it was not possible to generate any reasonable structure for DFT calculations starting from the putative bioactive conformers of **10b**, in agreement with its lack of antimalarial activity (Table 2).When the alkyl chain is moved from C3 to C6, the resulting compounds were overall less active, regardless of their relative stereochemistry (**11a−d**, Table 2). According to our DFT calculations, the methoxy group in the axial position, as in compounds **11a,b**, still drives the formation of the energetically favored O1/O2/O7 complex, with the consequent preferential formation of the radical on O2, but in this case, the hypothesized 1,4-H-shift can only occur at the C6 butyl chain. Assuming the formation of the radical on O2, the H-shift might involve the C6 butyl chain in axial position (**11b**) but not in equatorial position (**11a**). However, similar to what was observed for plakortins,[14] when the radical is formed on O2, the shift on C6 alkyl chain is hampered by O1−O2 separation and the consequent opening of the ring. Thus, the hypothesized "bioactive" reaction can only proceed through the thermodynamically unfavored formation of the O1 radical, in agreement with the same low antimalarial activity exhibited by **11a,b** (Table 2). On the other hand, when the methoxy group is in the equatorial position, as in compounds **11c,d**, the radical shift from O1 to C6 butyl chain is allowed by the formation of the O2/O7 complex (Figure 6c), and accordingly, **11c,d** are not as inactive as **10b** (Table 2). However, the O2/O7 prereactive complex is characterized by a weaker binding energy with respect to the O1/O2/O7 complex formed by **10a** (ΔE = 10 kcal/mol; Figure 6a,c). Accordingly, the antimalarial activity of **11c,d** is significantly lower than that of **10a** (Table 2).

Our computational results also seem to account for observed SARs of **8−14** when a butyl chain is present either at C3 or at C6 (**12a−c**, Table 2). Compounds **12a** and **12b**, bearing as **10a** the methoxy group in the axial position, were equally potent as **10a**. Indeed, they are all able to form the energetically favored O1/O2/O7 complex, driving the formation of the O2 radical, which in turn can shift on the C3 butyl chain, following the scheme reported in Figure 7. On the contrary, the equatorial position of the methoxy group at C3 in **12c**, as in **10b**, does not allow the energetically favored formation of the tricoordinated iron complex, as well as any "bioactive" reaction with C3 alkyl chain. Therefore, the activity is only due to the alkyl chain at C6 and **12c** showed, indeed, the same low antimalarial activity as compounds **11a−d** (Table 2).

Finally, important evidence of the hypothesized antimalarial mechanism is the SARs obtained when the number of the butyl chains at C6 is doubled (**13a,b**, **14a,b**). Indeed, according to the H-shift mechanism, entropic effects, ideally represented by increased occurrence of putative bioactive conformations reported in Table 5, account for the improved antimalarial activity of **13a,b** with respect to **11a−d** (Table 2). In line with these results, compounds **14a,b**, bearing two butyl chain at C6 and one butyl chain at C3, are equally active despite their different relative stereochemistry (Table 2), contrary to what happened for C6 monobutyl compounds **12a−c**. Indeed, the activity of **14a** is due to the C3 butyl chain, as for **10a** and **12a,b**, while the activity of **14b** is essentially due to the butyl chains at C6, as for **13b** (Table 2). It is noteworthy that compound **9**, although presenting relevant putative bioactive conformations due to favorable steric effects (32%, Table 5), showed no antimalarial activity (Table 2). This can be explained by considering that the putative toxic species responsible for antimalarial activity is, in the case of **9**, a primary carbon radical whose formation is thermodynamically less favored than the formation of a secondary carbon radical, as in the case of compounds bearing butyl chain(s).

CONCLUSIONS

Our results indicate that the ability to form a carbon centered radical on the alkyl chain installed on C3 and/or C6 of compounds **8**−**14** is related to their antimalarial activity. Computational and SAR studies suggest that, as in the case of plakortins, the putative toxic carbon radical species is formed through an intramolecular hydrogen shift. The presence of the methoxy group at C3 drives radical formation, resulting in stricter stereochemical requirements for antimalarial activity compared to plakortins. Nevertheless, our study demonstrated that, according to the hypothesized mechanism of action, the antimalarial activity can be improved through rational structural modifications, thus disclosing the antimalarial potential of the new 3-methoxy-1,2-dioxane scaffold, obtained by means of an efficient and cheap two-pot Mn(III)-mediated synthesis. As an example, compound **13b**, bearing two *n*-butyl substituents at C6, showed antimalarial activity against CQ-R strains comparable to plakortin and no significant toxicity against HMEC-1 cells.

EXPERIMENTAL SECTION

General Chemical Procedures. Low- and high-resolution ESI-MS spectra were performed on a LTQ Orbitrap XL (Thermo Scientific) mass spectrometer. ^{1}H (500 MHz) and ^{13}C (125 MHz) NMR spectra were measured on a Varian INOVA spectrometer. Chemical shifts were referenced to the residual solvent signal ($CDCl_3$: δ_H 7.26, δ_C 77.0). Homonuclear ^{1}H connectivities were determined by COSY experiments. One-bond heteronuclear ^{1}H−^{13}C connectivities were determined with HSQC experiments. Two- and three-bond ^{1}H−^{13}C connectivities were determined by HMBC experiments optimized for a $^{2,3}J$ of 7 Hz. Through-space ^{1}H connectivities were determined using ROESY with a mixing time of 250 ms. Two- and three-bond ^{1}H−^{13}C connectivities were determined by gradient 2D HMBC experiments optimized for a $^{2,3}J$ of 7 Hz. Reactions were monitored by TLC on Merck 60 F_{254} (0.25 mm) plates, which were visualized by UV inspection and/or staining with 5% H_2SO_4 in ethanol and heating. A Knauer HPLC apparatus equipped with refraction index detector was used to purify and assess purity (>95%) of all final products. LUNA (normal phase) (Phenomenex) columns were used, eluting with EtOAc/*n*-hexane mixtures at a flow rate of 0.7 mL/min.

Synthesis of 3-Hydroxy-1,2-dioxanes 5. General Procedure. The appropriate alkene (1 mmol) was added at room temperature to a mixture of the desired *β*-ketoester (3 mmol), $Mn^{III}(OAc)_3{\cdot}2H_2O$ (0.1 mmol, 0.027 g), and $Mn^{II}(OAc)_2{\cdot}4H_2O$ (1 mmol, 0.245 g) in acetic acid (5 mL). In the case of gaseous isobutylene (2-methylpropene), an excess of alkene was bubbled at −10 °C to a mixture of the desired *β*-ketoester (3 mmol), $Mn^{III}(OAc)_3{\cdot}2H_2O$ (0.1 mmol, 0.027 g), and $Mn^{II}(OAc)_2{\cdot}4H_2O$ (1 mmol, 0.245 g) in acetic acid (5 mL). The resulting heterogeneous solution was stirred at room temperature for 18−24 h under oxygen at atmospheric pressure (O_2 filled balloon), and the conversion was monitored by TLC. The reaction mixture was neutralized with stoichiometric NaOH (3 M aqueous solution) and then made slightly basic with a saturated $NaHCO_3$ solution. The aqueous phase was extracted with CH_2Cl_2 (3 × 10 mL) and the combined organic phases were dried (Na_2SO_4) and evaporated to dryness. The intermediate 3-hydroxy-1,2-dioxanes **5** were purified by flash chromatography on silica gel, eluting with cyclohexane/ethyl acetate mixtures.

Synthesis of 3-Methoxy-1,2-dioxanes 8−14. General Procedure. (1*S*)-(+)-Camphorsulfonic acid (5 mmol, 1.16 g) was added at room temperature to a solution of the desired 3-hydroxy-1,2-dioxane **5** (1 mmol) and trimethyl orthoformate (2 mmol, 0.22 mL) in anhydrous methanol (7 mL), and the solution was stirred at room temperature for 72 h. The reaction was quenched at 0 °C with saturated $NaHCO_3$ solution, and the aqueous phase was extracted with CH_2Cl_2 (3 × 10 mL). The combined organic phases were dried (Na_2SO_4) and evaporated to dryness. 3-Methoxy-1,2-dioxanes **8**−**14** were isolated after flash chromatography on silica gel by elution with cyclohexane/ethyl acetate mixtures.

Compound 8. ESI-MS: *m*/*z* 241 [M + Na]$^+$. HR ESI-MS: *m*/*z* 241.1059 (calcd for $C_{10}H_{18}NaO_5$ 241.1052). ^{1}H NMR (500 MHz): δ 3.72 (s, COOMe), 3.32 (s, OMe-3), 2.86 (dd, *J* = 12.9, 4.9 Hz, H-4), 2.26 (t, *J* = 12.9 Hz, H-5a), 1.59 (dd, *J* = 12.9, 4.9 Hz, H-5b), 1.47 (s, Me-3), 1.36 (s, Me-6ax), 1.21 (s, Me-6eq). ^{13}C NMR (125 MHz): δ 171.3 (COOMe), 100.4 (C-3), 77.1 (C-6), 51.9 (COOMe), 49.1 (OMe-3), 45.7 (C-4), 32.7 (C-5), 27.2 (6-Me), 22.3 (6-Me), 19.6 (3-Me).

Compound 9. ESI-MS: *m*/*z* 255 [M + Na]$^+$. HR ESI-MS: *m*/*z* 255.1212 (calcd for $C_{11}H_{20}NaO_5$ 255.1218). ^{1}H NMR (500 MHz): δ 3.80 (s, COOMe), 3.31 (s, OMe-3), 3.10 (dd, *J* = 12.9, 4.9 Hz, H-4), 2.30 (t, *J* = 12.9 Hz, H-5a), 1.90 (q, *J* = 7.2 Hz, H_2-1′), 1.59 (dd, *J* = 12.9, 4.9 Hz, H-5b), 1.36 (s, Me-6ax), 1.21 (s, Me-6eq), 1.03 (t, *J* = 7.2 Hz, H_2-2′). ^{13}C NMR (125 MHz): δ 171.4 (COOMe), 102.3 (C-3), 77.1 (C-6), 52.0 (COOMe), 51.9 (OMe-3), 48.6 (C-4), 40.4 (C-1′), 32.6 (C-5), 26.8 (6-Me), 22.6 (6-Me), 8.5 (C-2′).

Compound 10a. ESI-MS: *m*/*z* 283 [M + Na]$^+$. HR ESI-MS: *m*/*z* 283.1517 (calcd for $C_{13}H_{24}NaO_5$ 283.1521). ^{1}H NMR (500 MHz): δ 3.71 (s, COOMe), 3.31 (s, OMe-3), 3.08 (dd, *J* = 12.9, 4.9 Hz, H-4), 2.29 (t, *J* = 12.9 Hz, H-5a), 1.86 (m, H-1′a), 1.58 (dd, *J* = 12.9, 4.9 Hz, H-5b), 1.34 (s, Me-6ax), 1.54 (m, H_2-2′), 1.34 (m, H_2-3′), 1.20 (s, Me-6eq), 0.92 (t, *J* = 6.9 Hz, H_3-4′). ^{13}C NMR (125 MHz): δ 171.4 (COOMe), 102.3 (C-3), 65.8 (C-6), 52.0 (COOMe), 52.0 (OMe-3), 48.6 (C-4), 40.4 (C-1′), 32.6 (C-5), 32.2 (C-2′), 26.8 (6-Me), 22.6 (6-Me), 21.0 (C-3′), 13.5 (C-4′).

Compound 10b. ESI-MS: *m*/*z* 283 [M + Na]$^+$. HR ESI-MS: *m*/*z* 283.1522 (calcd for $C_{13}H_{24}NaO_5$ 283.1521). ^{1}H NMR (500 MHz): δ 3.73 (s, COOMe), 3.41 (s, OMe-3), 3.06 (dd, *J* = 13.0, 5.5 Hz, H-4), 1.89 (m, H-1′a), 1.85 (dd, *J* = 13.0, 5.5 Hz, H-5a), 1.72 (t, *J* = 13.0 Hz, H-5b), 1.54 (m, H_2-2′),1.37 (s, Me-6ax), 1.34 (m, H_2-3′), 1.19 (s, Me-6eq), 0.92 (t, *J* = 6.9 Hz, H_3-4′). ^{13}C NMR (125 MHz): δ 173.4 (COOMe), 104.2 (C-3), 73.8 (C-6), 52.5 (COOMe), 52.0 (OMe-3), 49.3 (C-4), 40.4 (C-1′), 35.6 (C-5), 32.2 (C-2′), 27.1 (6-Me), 21.6 (6-Me), 21.0 (C-3′), 13.5 (C-4′).

Compound 11a. ESI-MS: *m*/*z* 283 [M + Na]$^+$. HR ESI-MS: *m*/*z* 283.1519 (calcd for $C_{13}H_{24}NaO_5$ 283.1521). ^{1}H NMR (500 MHz): δ 3.70 (s, COOMe), 3.30 (s, OMe-3), 2.85 (dd, *J* = 12.5, 6.4 Hz, H-4), 2.22 (dd, *J* = 12.0, 12.0 Hz, H-5a), 1.53 (dd, *J* = 12.0, 6.4 Hz, H-5b), 1.50 (m, H_2-1′), 1.35 (m, H_2-2′), 1.30 (m, H_2-3′), 1.47 (s, Me-3), 1.32 (s, Me-6), 0.93 (t, *J* = 6.9 Hz, H_3-4′).

Compound 11b. ESI-MS: *m*/*z* 283 [M + Na]$^+$. HR ESI-MS: *m*/*z* 283.1529 (calcd for $C_{13}H_{24}NaO_5$ 283.1521). ^{1}H NMR (500 MHz): δ 3.70 (s, COOMe), 3.30 (s, OMe-3), 2.84 (dd, *J* = 12.5, 6.4 Hz, H-4), 2.22 (dd, *J* = 12.0, 12.0 Hz, H-5a), 1.80 (m, H_2-1′), 1.64 (dd, *J* = 12.0, 6.4 Hz, H-5b), 1.55 (m, H_2-2′), 1.30 (m, H_2-3′), 1.45 (s, Me-3), 1.13 (s, Me-6), 0.93 (t, *J* = 6.9 Hz, H_3-4′). ^{13}C NMR (125 MHz): δ 171.5 (COOMe), 100.1 (C-3), 79.9 (C-6), 52.5 (COOMe), 49.1 (OMe-3), 45.5 (C-4), 33.9 (C-1′), 31.2 (C-5), 26.1 (C-2′), 23.9 (Me-6), 23.1 (C-3′), 19.5 (Me-3), 14.7 (C-4′).

Compound 11c. ESI-MS: *m*/*z* 283 [M + Na]$^+$. HR ESI-MS: *m*/*z* 283.1530 (calcd for $C_{13}H_{24}NaO_5$ 283.1521). ^{1}H NMR (500 MHz): δ 3.73 (s, COOMe), 3.38 (s, OMe-3), 2.98 (dd, *J* = 11.1, 6.4 Hz, H-4), 1.77 (m, H_2-5), 1.59 (m, H_2-1′), 1.34 (m, H_2-2′ and H_2-3′), 1.25 (s, Me-3), 1.12 (s, Me-6), 0.93 (t, *J* = 6.9 Hz, H_3-4′). ^{13}C NMR (125 MHz): δ 173.2 (COOMe), 105.7 (C-3), 82.1 (C-6), 52.5 (COOMe), 50.3 (OMe-3), 47.3 (C-4), 39.9 (C-5), 34.4 (C-1′), 26.1 (C-2′), 23.6 (C-3′), 20.6 (Me-6), 17.8 (Me-3), 14.7 (C-4′).

Compound 11d. ESI-MS: *m*/*z* 283 [M + Na]$^+$. HR ESI-MS: *m*/*z* 283.1512 (calcd for $C_{13}H_{24}NaO_5$ 283.1521). ^{1}H NMR (500 MHz): δ 3.73 (s, COOMe), 3.38 (s, OMe-3), 2.98 (dd, *J* = 13.8, 3.8 Hz, H-4), 1.89 (dd, *J* = 14.0, 3.4 Hz, H-5a), 1.69 (dd, *J* = 14.0, 12.5 Hz, H-5b), 1.45 (m, H_2-1′), 1.32 (s, Me-6), 1.29 (m, H_2-2′ and H_2-3′), 1.26 (s, Me-3), 0.89 (t, *J* = 6.9 Hz, H_3-4′). ^{13}C NMR (125 MHz): δ 172.8 (COOMe), 105.7 (C-3), 82.1 (C-6), 52.0 (COOMe), 50.3 (OMe-3), 46.9 (C-4), 36.3 (C-5), 33.4 (C-1′), 26.0 (C-2′), 23.4 (C-3′), 20.6 (Me-6), 17.1 (Me-3), 14.3 (C-4′).

Compound 12a. ESI-MS: *m*/*z* 325 [M + Na]$^+$. HR ESI-MS: *m*/*z* 325.2000 (calcd for $C_{16}H_{30}NaO_5$ 325.1991). ^{1}H NMR (500 MHz):

dx.doi.org/10.1021/jm201056j | J. Med. Chem. 2011, 54, 8526−8540

δ 3.71 (s, COOMe), 3.31 (s, OMe-3), 3.07 (dd, J = 12.9, 4.5 Hz, H-4), 2.23 (t, J = 12.9 Hz, H-5a), 1.85 (m, H-1′a), 1.80 (m, H-1″a), 1.79 (m, H-1′a), 1.70 (m, H-1″b), 1.62 (overlapped, H-5b), 1.59 (m, H_2-2′ and H_2-2″), 1.34 (m, H_2-3′ and H_2-3″), 1.30 (s, Me-6), 0.93 (t, J = 6.9 Hz, H_3-4′ and H_3-4″).

Compound 12b. ESI-MS: m/z 325 $[M + Na]^+$. HR ESI-MS: m/z 325.1987 (calcd for $C_{16}H_{30}NaO_5$ 325.1991). ^{1}H NMR (500 MHz): δ 3.71 (s, COOMe), 3.31 (s, OMe-3), 3.07 (dd, J = 12.9, 4.5 Hz, H-4), 2.23 (t, J = 12.9 Hz, H-5a), 1.92 (m, H-1′a), 1.83 (m, H-1″a), 1.82 (m, H-1′b), 1.70 (m, H-1″b), 1.64 (dd, J = 12.9, 4.5 Hz, H-5b), 1.54 (m, H_2-2′ and H_2-2″), 1.34 (m, H_2-3′ and H_2-3″), 1.13 (s, Me-6), 0.93 (t, J = 6.9 Hz, H_3-4′ and H_3-4″). ^{13}C NMR (125 MHz): δ 171.5 (COOMe), 102.0 (C-3), 79.1 (C-6), 51.8 (COOMe), 48.6 (OMe-3), 40.6 (C-4), 34.0 (C-5), 33.9 (C-1′), 32.5 (C-1″), 31.4 (C-2′), 29.7 (C-2″), 26.1 (C-3′), 25.8 (C-3″), 23.0 (Me-6), 14.0 (C-4′), 13.8 (C-4″).

Compound 12c. ESI-MS: m/z 325 $[M + Na]^+$. HR ESI-MS: m/z 325.1993 (calcd for $C_{16}H_{30}NaO_5$ 325.1991). ^{1}H NMR (500 MHz): δ 3.73 (s, COOMe), 3.41 (s, OMe-3), 3.07 (dd, J = 12.9, 4.5 Hz, H-4), 1.92 (m, H-1′a), 1.83 (m, H-1″a, H-1′b), 1.77 (m, H_2-5), 1.70 (m, H-1″b), 1.54 (m, H_2-2′ and H_2-2″), 1.34 (m, H_2-3′ and H_2-3″), 1.11 (s, Me-6), 0.93 (t, J = 6.9 Hz, H_3-4′ and H_3-4″).

Compound 13a. ESI-MS: m/z 325 $[M + Na]^+$. HR ESI-MS: m/z 325.1988 (calcd for $C_{16}H_{30}NaO_5$ 325.1991). ^{1}H NMR (500 MHz): δ 3.71 (s, COOMe), 3.31 (s, OMe-3), 2.83 (dd, J = 12.9, 4.5 Hz, H-4), 2.21 (t, J = 12.9 Hz, H-5a), 1.82 (m, H-1″a), 1.81 (m, H-1′a), 1.60 (dd, J = 12.9, 4.5 Hz, H-5b), 1.60 (m, H-1″b, H-1′b), 1.54 (m, H_2-2′ and H_2-2″), 1.45 (s, Me-3), 1.34 (m, H_2-3′ and H_2-3″), 0.91 (t, J = 6.9 Hz, H_3-4′ and H_3-4″). ^{13}C NMR (125 MHz): δ 171.5 (COOMe), 100.5 (C-3), 81.0 (C-6), 51.8 (COOMe), 49.0 (OMe-3), 45.1 (C-4), 36.1 (C-5), 31.3 (C-1′), 29.6 (C-1″), 25.4 (C-2′), 24.8 (C-2″), 23.2 (Me-3), 19.6 (C-3′, C-3″), 14.0 (C-4′), 13.9 (C-4″).

Compound 13b. ESI-MS: m/z 325 $[M + Na]^+$. HR ESI-MS: m/z 325.1995 (calcd for $C_{16}H_{30}NaO_5$ 325.1991). ^{1}H NMR (500 MHz): δ 3.74 (s, COOMe), 3.40 (s, OMe-3), 3.00 (dd, J = 13.5, 3.5 Hz, H-4), 1.84 (dd, J = 13.5, 3.5 Hz, H-5a), 1.72 (t, J = 13.5, H-5b), 1.65 (m, H-1″a), 1.60 (m, H-1′a), 1.57 (s, Me-3), 1.45 (m, H-1″b, H-1′b), 1.39 (m, H_2-2′ and H_2-2″), 1.34 (m, H_2-3′ and H_2-3″), 0.93 (t, J = 6.9 Hz, H_3-4′), 0.90 (t, J = 6.9 Hz, H_3-4″). ^{13}C NMR (125 MHz): δ 172.6 (COOMe), 105.5 (C-3), 83.8 (C-6), 52.0 (COOMe), 49.6 (OMe-3), 46.4 (C-4), 36.7 (C-5), 32.6 (C-1′), 32.4 (C-1″), 26.2 (Me-3), 25.4 (C-2′), 25.2 (C-2″), 23.2 (C-3′) 23.1 (C-3″), 14.0 (C-4′), 13.9 (C-4″).

Compound 14a. ESI-MS: m/z 367 $[M + Na]^+$. HR ESI-MS: m/z 367.2467 (calcd for $C_{19}H_{36}NaO_5$ 367.2460). ^{1}H NMR (500 MHz): δ 3.71 (s, COOMe), 3.30 (s, OMe-3), 3.10 (dd, J = 12.9, 4.5 Hz, H-4), 2.21 (t, J = 12.9 Hz, H-5a), 1.87 (m, H_2-1′), 1.78 (m, H_2-1″, H_2-1‴), 1.60 (dd, J = 12.9, 4.5 Hz, H-5b), 1.49 (m, H_2-2′ and H_2-2″), 1.25 −1.35 (m, H_2-2‴, H_2-3′ H_2-3″, H_2-3‴), 0.91 (t, J = 6.9 Hz, H_3-4′ H_3-4″, H_3-4‴). ^{13}C NMR (125 MHz): δ 171.6 (COOMe), 102.1 (C-3), 81.0 (C-6), 51.8 (COOMe), 48.6 (OMe-3), 44.2 (C-4), 32.9 (C-1′), 32.6 (C-1″), 31.3 (C-5), 26.1 (C-2′ and C-2″), 23.2 (Me- 3), 23.1 (C-3′ and C-3″), 13.9 (C-4′ and C-4″).

Compound 14b. ESI-MS: m/z 367 $[M + Na]^+$. HR ESI-MS: m/z 367.2452 (calcd for $C_{19}H_{36}NaO_5$ 367.2460). ^{1}H NMR (500 MHz): δ 3.71 (s, COOMe), 3.30 (s, OMe-3), 3.07 (dd, J = 12.9, 3.5 Hz, H-4), 1.85 (dd, J = 12.9, 3.5 Hz, H-5a), 1.72 (t, J = 12.9 Hz, H-5b), 1.65 (m, H_2-1′), 1.60−1.63 (m, H_2-1″, H_2-1‴), 1.40−1.20 (m, H_2-2′, H_2-2″, H_2-2‴, H_2-3′ H_2-3″, H_2-3‴), 0.89 (t, J = 6.9 Hz, H_3-4′ H_3-4″, H_3-4‴). ^{13}C NMR (125 MHz): δ 172.8 (COOMe), 106.1 (C-3), 83.5 (C-6), 52.0 (COOMe), 50.0 (OMe-3), 44.2 (C-4), 36.6 (C-1′), 36.1 (C-1″), 30.5 (C-5), 29.6 (C-2′ and C-2″), 25.3 (Me- 3), 24.5 (C-3′ and C-3″), 13.8 (C-4′ and C-4″).

Reaction of Methylketals with $FeCl_2$. Compound **12b** (12.0 mg, 0.040 mmol) was dissolved in CH_3CN/H_2O, 4:1 (5 mL), and freshly purchased $FeCl_2.4H_2O$ (39 mg, 0.20 mmol) was added. The reaction mixture was left under stirring at room temperature for 2 h. Light was excluded from the reaction. Then the obtained mixture was partitioned between water and EtOAc. The organic phase, dried over Na_2SO_4, was purified by HPLC (SI60 *n*-hexane/EtOAc, 85:15), affording compound **15** (2.7 mg, 0.0124 mmol, 31%) in the pure state. When the reaction was repeated with compounds **9** and **10b**, in the same conditions, compound **16** (45% and 42% yield, respectively) was obtained.

Compound 15. ESI-MS: m/z 237 $[M + Na]^+$. HR ESI-MS: m/z 237.1100 (calcd for $C_{11}H_{18}NaO_4$ 237.1103). ^{1}H NMR (500 MHz): δ 4.12 (m, H-2), 3.90 (s, 9-OMe), 2.60 (dd, J = 11.5, 4.5 Hz, H-3a), 2.40 (dd, J = 11.5, 6.0 Hz, H-3b), 1.85 (m, H-5a), 1.70 (m, H-5b), 1.60 (s, Me-10), 1.50 (m, H_2-6), 1.30 (m, H_2-7), 0.93 (t, J = 7.2 Hz, Me-8). ^{13}C NMR (125 MHz): δ 171.0 (C-1), 169.5 (COO-), 83.9 (C-4), 51.0 (OMe), 48.5 (C-2), 38.3 (C-5), 36.6 (C-3), 23.8 (C-6), 23.5 (C-10), 23.0 (C-7), 14.0 (C-8).

Compound 16. ESI-MS: m/z 195 $[M + Na]^+$. HR ESI-MS: m/z 195.0639 (calcd for $C_8H_{12}NaO_4$ 195.0633). ^{1}H NMR (500 MHz): δ 3.90 (s, COOMe), 3.73 (t, J = 6.0 Hz, H-2), 2.55 (dd, J = 11.5, 4.5 Hz, H-3a), 2.32 (dd, J = 11.5, 8.0 Hz, H-3b), 1.53 (s, H_3-5), 1.42 (s, H_3-6). ^{13}C NMR (125 MHz): δ 171.0 (C-1), 168.5 (COO-), 83.7 (C-4), 51.0 (OMe), 47.7 (C-2), 38.2 (C-3), 28.3 (C-5), 27.8 (C-6).

Molecular Modeling. Molecular modeling calculations were performed on SGI Origin 200 8XR12000 and E4 Server Twin 2× Dual Xeon-5520, equipped with two nodes. Each node had the following: 2× Intel Xeon QuadCore E5520, 2.26 GHz, 36 GB RAM. The molecular and graphics modeling was carried out on SGI Octane 2 workstations.

The apparent pK_a and log D (pH 7.4) of the newly designed compounds **8**−**14** were calculated by using the ACD/pKa DB, version 12.00, software (Advanced Chemistry Development Inc., Toronto, Canada). All compounds were considered neutral in all calculations performed as a consequence of the estimation of percentage of neutral/ionized forms computed at pH 7.4 (physiological value), pH 7.2 (cytoplasmic value), and pH 5.5 (parasite vacuole value) using the Handerson−Hasselbalch equation.

Conformational Analysis. Compounds **8**−**14** were built using the Insight 2005 Builder module (Accelrys Software Inc., San Diego, CA). Atomic potentials and charges were assigned using the CFF91 force field.[43]

The conformational space of compounds was sampled through 200 cycles of simulated annealing (ε = 1). In simulated annealing, the temperature is altered in time increments from an initial temperature to a final temperature by adjusting the kinetic energy of the structure (by rescaling the velocities of the atoms). The following protocol was applied: the system was heated to 1000 K over 2000 fs (time step of 3.0 fs); a temperature of 1000 K was applied to the system for 2000 fs (time step of 3.0 fs) to surmount torsional barriers; successively, temperature was linearly reduced to 300 K in 1000 fs (time step of 1.0 fs). Resulting conformations were then subjected to MM energy minimization within Insight 2005 Discover module (CFF91 force field (ε = 1) until the maximum rmsd was less than 0.001 kcal/Å, using conjugate gradient[44] as the minimization algorithm. In order to evaluate the effects of the implicit solvent, we sampled the conformational space of **10a** through the combined procedure of simulated annealing/MM calculations, using also the dielectric constant of the water (ε = 80r). All MM conformers were then subjected to a full geometry optimization by semiempirical calculations, using the quantum mechanical method PM6[45] in the MOPAC2009 package[46] and EF[47] (eigenvector following routine) as geometry optimization algorithm. GNORM value was set to 0.01. To reach a full geometry optimization, the criterion for terminating all optimizations was increased by a factor of 100, using the keyword PRECISE.

Resulting conformers were grouped into families on the basis of their 1,2-dioxane ring conformations and ranked by their potential energy values (i.e., ΔE from the global energy minimum). Occurrence rates, together with the distance between endoperoxide oxygens (O1 and O2) and possible partners for a "through space" (1,4 and 1,5) intramolecular radical shift, were calculated for all conformers within 5 kcal/mol from the global minimum. The accessible surface area of endoperoxide oxygens lone pairs has been evaluated by calculating Connolly surfaces (Insight 2005, Accelrys Software Inc., San Diego, CA).

Docking Procedure. In order to find the bioactive conformation, docking studies were carried out on newly designed compounds in

complex with heme, using a docking methodology (Affinity, SA_Docking; Insight 2005, Accelrys, San Diego, CA) which considers all the systems flexible (i.e., ligand and target). Atomic potentials were assigned using the Heme29.frc;[48] a force field including heme parameters and atomic partial charges were assigned using PM6.[45] Heme apparent pK_a values were calculated by using the ACD/pKa DB, version 12.00, software (Advanced Chemistry Development Inc., Toronto, Canada). Accordingly, one propionic chain was considered protonated and the heme net total charge was set at +1.

Although during the subsequent dynamic docking protocol all the systems were perturbed by means of Monte Carlo and simulated annealing procedures, a reasonable starting structure is anyway required. Thus, the PM6 lowest energy conformer meeting the hypothesized pharmacophoric requirements for antimalarial activity was selected as the ligand starting conformation. The ligands were then placed above the heme, taking as template the crystal structure of a peroxo-bridged heme−copper dinuclear complex (CSD code UKACIS). All atoms in the complex were left free to move during the entire docking calculations with the exception of heme pyrrolic carbons, which were kept fixed. The Cell_Multipole method[49] has been used to calculate nonbond interactions. A Monte Carlo/minimization approach for the random generation of a maximum of 20 acceptable ligand/heme complexes, for each compound, was used. During the first step, starting from the previously obtained roughly docked structures, the ligand was moved by a random combination of translation, rotation, and torsional changes (Flexible_Ligand option, considering all rotatable bonds) to sample both the conformational space of the ligand and its orientation with respect to the heme (MxRChange = 3 Å; MxAngChange = 180°). During this step, van der Waals (vdW) and Coulombic terms were scaled to a factor of 0.1 to avoid very severe divergences in the Coulombic and vdW energies. If the energy of a complex structure resulting from random moves of the ligand was higher by the energy tolerance parameter than the energy of the last accepted structure, it was not accepted for minimization. To ensure a wide variance of the input structures to be successively minimized, an energy tolerance value of 10^6 kcal mol^{-1} from the previous structure has been used. After the energy minimization step (conjugate gradient, 2500 iterations, $\varepsilon = 1$), the Metropolis test, at a temperature of 310 K, and a structure similarity check (rms tolerance of 0.3 kcal Å^{-1}) were applied to select the 20 acceptable structures. Each subsequent structure was generated from the last accepted structure. All the accepted complexes resulting from the Monte Carlo/minimization approach were subjected to a molecular dynamics simulated annealing protocol, including 5 ps of a dynamic run divided in 50 stages (100 fs each) during which the temperature of the system was linearly decreased from 500 to 300 K (Verlet velocity integrator; time step of 1.0 fs). Molecular dynamics calculations were performed using a constant temperature and constant volume (*NVT*) statistical ensemble, and the direct velocity scaling as temperature control method (temp window, 10 K). In the first stage, initial velocities were randomly generated from the Boltzmann distribution according to the desired temperature, while during the subsequent stages initial velocities were generated from dynamics restart data. A temperature of 500 K was applied to surmount torsional barriers, thus allowing an unconstrained rearrangement of the ligand and the heme (initial vdW and Coulombic scale factors of 0.1). Successively temperature was linearly reduced to 300 K in 5 ps, and concurrently the scale factors have been similarly decreased from their initial values (0.1) to their final values (1.0). A final round of 10^4 minimization steps (conjugate gradient, $\varepsilon = 1$) followed the last dynamics steps, and the minimized structures were saved in a trajectory file. After this procedure, the resulting docked structures were ranked by their conformational energy and the geometry of endoperoxide−iron coordination bond. The ligand−heme interaction energy of each complex was evaluated by calculating (i) the total energy between the ligand and the heme, using the Evaluate command in the Docking module of Insight 2005 (vdW and electrostatic energy contribution, no CUT_OFF), and (ii) the nonbond interaction energy between the ligand and the heme, using the Discover_3 Module of Insight 2005 (vdW and electrostatic energy contribution, no CUT_OFF). The complex showing the higher binding energy, the best iron coordination geometry (lowest rmsd fitted on experimental data, CSD code UKACIS), and the correct orientation of the pharmacophoric features was selected as the putative bioactive conformation and was then subjected to DFT calculations.

Density Functional Calculations. All calculations were carried out using the Gaussian 09 package.[50] The 3D spin density isosurface plots were visualized by Gabedit 2.3.5 software.[51] The theoretical protocol used includes Becke (B3) exchange[52] and Lee, Yang, and Parr (LYP) correlation potentials[53] in connection with 6-311++G** basis set functions for non-metal atoms.[54] The presence of diffuse functions ensures a proper description for the anionic species molecular orbitals. An all-electron orbital basis set built ad hoc to improve B3LYP performances in the treatment of metals, DZVP (opt), was used for iron.[55] It is noteworthy that the combination of a hybrid exchange-correlation functional as B3LYP with an all-electron basis set for the metal instead of a pseudopotential[56] allows a correct representation of spin density distribution. All stationary points were optimized without any geometrical constraints. Vibrational analysis was carried out at the same level of theory (i) to identify O1−O2 stretching modes, (ii) to characterize every compound as minimum or transition state on the potential energy surface, and (iii) to obtain zero point energy correction.

To corroborate the hypothesized reaction mechanism with the aim to help the drug design process, the negative charge and the unpaired electron were localized on the molecular system. Since the reduction of the endoperoxide by Fe(II) is a dissociative electron transfer (DET), then the derived species is a radical anion. This latter is characterized by just one unpaired electron; consequently, the multiplicity was set to doublet and the charge to −1 . To model the iron/endoperoxide complex, all possible Fe(II) and Fe(III) coordination geometries were used as starting structures for the DFT study. The analysis of APT charges, Mulliken spin density, and NBO spin density isosurfaces was evaluated on every structure. It is in fact well-known that both methods ensure obtaining of reliable data of spin population,[57] and our aim was to compare the results derived from both approaches.

The radical shift from the endoperoxide oxygen to the alkyl chain carbon was analyzed by tracing the reaction path of the process involving **10a**. The initial structure of the transition state was obtained by the QST2 method.[58] Besides charges and spin density distribution analysis on all stationary points, the intrinsic reaction coordinate (IRC) methodology was used to undoubtedly identify the transition state on the potential energy surface.[59]

In order to evaluate any possible conformational change due to the solvent, a full optimization at the B3LYP/6-311++G**/PCM level was carried out on the bioactive conformation of **10a**. The SCRF/PCM method allows the calculation of the energy in the presence of a solvent. In this case **10a** was optimized as a solute in an aqueous solution. In detail, the solute is included in a cavity within the solvent reaction field. By this approach, the solute cavity is obtained through a set of overlapping spheres.

In Vitro Drug Susceptibility Assay on *P. falciparum*. *Plasmodium falciparum* cultures were carried out according to Trager and Jensen with slight modifications.[60] The CQ-S, strain D10, and the CQ-R, strain W2, were maintained at 5% hematocrit (human type A-positive red blood cells) in RPMI 1640 (EuroClone, Celbio) medium with the addition of 1% AlbuMax (Invitrogen, Milan, Italy), 0.01% hypoxanthine, 20 mM Hepes, and 2 mM glutamine. All the cultures were maintained at 37 °C in a standard gas mixture consisting of 1% O_2, 5% CO_2, and 94% N_2. Compounds were dissolved in either water or DMSO and then diluted with medium to achieve the required concentrations (final DMSO concentration of <1%, which is nontoxic to the parasite). Drugs were placed in 96-well flat-bottomed microplates (COSTAR) and serial dilutions made. Asynchronous cultures with parasitemia of 1−1.5% and 1% final hematocrit were aliquoted into the plates and incubated for 72 h at 37 °C. Parasite growth was determined spectrophotometrically (OD_{650}) by measuring the activity of the parasite lactate dehydrogenase (pLDH) according to a modified version of the method of Makler in control and drug-treated cultures.[61] The antimalarial activity is expressed as 50%

dx.doi.org/10.1021/jm201056j | J. Med. Chem. 2011, 54, 8526−8540

inhibitory concentrations (IC_{50}); each IC_{50} value is the mean and standard deviation of at least three separate experiments performed in duplicate.

Cell Cytotoxicity Assays. The long-term HMEC-1 immortalized by SV 40 large T antigen[62] was maintained in MCDB 131 medium (Invitrogen, Milan, Italy) supplemented with 10% fetal calf serum (HyClone, Celbio, Milan, Italy), 10 ng/mL epidermal growth factor (Chemicon), 1 μg/mL hydrocortisone, 2 mM glutamine, 100 U/mL penicillin, 100 L μg/mL streptomycin, and 20 mM Hepes buffer (EuroClone). Unless stated otherwise, all reagents were from Sigma Italia, Milan, Italy. For the cytotoxicity assays, cells were treated with serial dilutions of test compounds and cell proliferation evaluated using the MTT assay already described.[63] Plates were incubated for 72 h at 37 °C in 5% CO_2. Then 20 μL of a 5 mg/mL solution of 3-(4,5-dimethylthiazol-2-yl)-2,5-diphenyltetrazolium bromide (MTT) (M-2128 Sigma) in PBS was added for an additional 3 h at 37 °C. The plates were then centrifuged, the supernatants discarded, and the dark blue formazan crystals dissolved using 100 μL of lysing buffer consisting of 20% (w/v) of a solution of SDS (Sigma), 40% of *N*,*N*-dimethylformamide (Merck) in H_2O, at pH 4.7 adjusted with 80% acetic acid. The plates were then read on a microplate reader (Molecular Devices Co., Menlo Park, CA, U.S.) at a test wavelength of 550 nm and a reference wavelength of 650 nm. The results are expressed as IC_{50}, which is the dose of compound necessary to inhibit cell growth by 50%. All the tests were performed in triplicate at least three times.[17]

■ ASSOCIATED CONTENT

Ⓢ Supporting Information

Calculated logD of new and reference compounds; APT charges, Mulliken spin densities values, and NBO spin density isosurfaces (B3LYP/6-311++G**) of **10a** radical anion; comparison of occurrence rates of low energy **10a** MM conformers using ε = 80*r or ε = 1; superimposition of **10a** DFT conformers in vacuo and in water; calculated vibrational modes of compounds **10a**; DFT starting structure of **10b**/(FeII)(O2/O7 coordination). This material is available free of charge via the Internet at http://pubs.acs.org.

■ AUTHOR INFORMATION

Corresponding Author

*For M.L.: phone, +390512099544; fax, +390512099456; e-mail, marco.lombardo@unibo.it. For C.F.: phone, +39081678544; fax, +39081678552; e-mail, caterina.fattorusso@unina.it.

Author Contributions

⊥These authors equally contributed to this work.

■ ACKNOWLEDGMENTS

This work was supported by MIUR (PRIN2008, Leads ad Attività Antimalarica di Origine Naturale, Isolamento, Ottimizzazione e Valutazione Biologica) and by the 7th Framework Programme of the European Community (Contract REGPOT-2008-1-NatPharma). MS and NMR spectra were recorded at the "Centro di Ricerca Interdipartimentale di Analisi Strumentale" of the University of Naples "Federico II", Italy. The University of Bologna, Italy, is acknowledged for financial support. Part of this manuscript was generated in the context of the AntiMal project, funded under the 6th Framework Programme of the European Community (Contract No. IP-018834). The authors are solely responsible for its content; it does not represent the opinion of the European Community, and the Community is not responsible for any use that might be made of the information contained herein. We thank the Associazione Volontari Italiani Sangue (AVIS Comunale Milano) for providing fresh red blood cells for *P. falciparum* growth.The assistance of the staff is gratefully acknowledged.

■ ABBREVIATIONS USED

CQ-R, chloroquine resistant; CQ-S, chloroquine sensitive; Pf, *Plasmodium falciparum*; DET, dissociative electron transfer; TPP, target product profile; MMV, Medicine for Malaria Venture; SERC, single exposure radical cure; HMEC-1, human microvascular endothelial cell line; SAR, structure−activity relationship; MM, molecular mechanics; MD, molecular dynamics; DFT, density functional theory; APT, atomic polar tensor; NBO, natural bond order; TS, transition state; EF, eigenvector following routine; vdW, van der Waals; LYP, Lee, Yang, and Parr; IRC, intrinsic reaction coordinate; pLDH, parasite lactate dehydrogenase

■ REFERENCES

(1) Wells, T. N. C. Natural products as starting points for future anti-malarial therapies: going back to our roots? *Malaria J.* **2011**, *10*, S1−S3.

(2) Arav-Boger, R.; Shapiro, T. A. Molecular mechanisms of resistance in antimalarial chemotherapy: the unmet challenge. *Annu. Rev. Pharmacol. Toxicol.* **2005**, *45*, 565−585.

(3) Li, Q.; Hickman, M. Toxicokinetic and toxicodynamic (TK/TD) evaluation to determine and predict the neurotoxicity of artemisinins. *Toxicology* **2011**, *279*, 1−9.

(4) Dondorp, A. M.; Yeung, S.; White, L.; Nguon, C.; Day, N. P. J.; Socheat, D.; von Seidlein, L. Artemisinin resistance: current status and scenarios for containment. *Nat. Rev. Microbiol.* **2010**, *8*, 272−280.

(5) Cafieri, F.; Fattorusso, E.; Taglialatela-Scafati, O.; Ianaro, A. Metabolites from the sponge *Plakortis simplex*. Determination of absolute stereochemistry of Plakortin. Isolation and stereostructure of three Plakortin related compounds. *Tetrahedron* **1999**, *55*, 7045−7056.

(6) Fattorusso, E.; Parapini, S.; Campagnuolo, C.; Basilico, N.; Taglialatela-Scafati, O.; Taramelli, D. Activity against *Plasmodium falciparum* of cycloperoxide compounds obtained from the sponge Plakortis simplex. *J. Antimicrob. Chemother.* **2002**, *50*, 883−888.

(7) Campagnuolo, C.; Fattorusso, E.; Romano, A.; Taglialatela-Scafati, O.; Basilico, N.; Parapini, S.; Taramelli, D. Antimalarial polyketide cycloperoxides from the marine sponge *Plakortis simplex*. *Eur. J. Org. Chem.* **2005**, 5077−5083.

(8) Fattorusso, E.; Taglialatela-Scafati, O.; Ianaro, A.; Di Rosa, M. Metabolites from the sponge *Plakortis simplex*. Part 3: Isolation and stereostructure of novel bioactive cycloperoxides and diol analogues. *Tetrahedron* **2000**, *56*, 7959−7967.

(9) Fattorusso, C.; Campiani, G.; Catalanotti, B.; Persico, M.; Basilico, N.; Parapini, S.; Taramelli, D.; Campagnuolo, C.; Fattorusso, E.; Romano, A.; Taglialatela-Scafati, O. Endoperoxide derivatives from marine organisms: 1,2-dioxanes of the plakortin family as novel antimalarial agents. *J. Med. Chem.* **2006**, *49*, 7088−7094.

(10) Haynes, R. K.; Chan, W.-C.; Wong, H.-N.; Li, K.-Y.; Wu, W.-K.; Fan, K.-M.; Sung, H. H. Y.; Williams, I. D.; Prosperi, D.; Melato, S.; Coghi, P.; Monti, D. Facile oxidation of leucomethylene blue and dihydroflavins by artemisinins: relationship with flavoenzyme function and antimalarial mechanism of action. *ChemMedChem* **2010**, *5*, 1282−1299.

(11) Mercer, A. E.; Copple, I. M.; Maggs, J. L.; O'Neill, P. M.; Park, B. K. The role of heme and the mitochondrion in the chemical and molecular mechanisms of mammalian cell death induced by the artemisinin antimalarials. *J. Biol. Chem.* **2011**, *286*, 987−996.

(12) O'Neill, P. M.; Posner, G. H. A medicinal chemistry perspective on artemisinin and related endoperoxides. *J. Med. Chem.* **2004**, *47*, 2945−2964.

(13) Posner, G. H.; O'Neill, P. M. Knowledge of the proposed chemical mechanism of action and cytochrome P450 metabolism of antimalarial trioxanes like artemisinin allows rational design of new antimalarial peroxides. *Acc. Chem. Res.* **2004**, *37*, 379−404.

(14) Taglialatela-Scafati, O.; Fattorusso, E.; Romano, A.; Scala, F.; Barone, V.; Cimino, P.; Stendardo, E.; Catalanotti, B.; Persico, M.; Fattorusso, C. Insight into the mechanism of action of plakortins, simple 1,2-dioxane antimalarials. *Org. Biomol. Chem.* **2010**, *8*, 846–856.
(15) Robert, A.; Benoit-Vical, F.; Meunier, B. The key role of heme to trigger the antimalarial activity of trioxanes. *Coord. Chem. Rev.* **2005**, *249*, 1927–1936.
(16) Fattorusso, C.; Persico, M.; Calcinai, B.; Cerrano, C.; Parapini, S.; Taramelli, D.; Novellino, E.; Romano, A.; Scala, F.; Fattorusso, E.; Taglialatela-Scafati, O. Manadoperoxides A–D from the Indonesian sponge *Plakortis* cfr. *simplex*. Further insights on the structure–activity relationships of simple 1,2-dioxane antimalarials. *J. Nat. Prod.* **2010**, *73*, 1138–1145.
(17) Fattorusso, C.; Persico, M.; Basilico, N.; Taramelli, D.; Fattorusso, E.; Scala, F.; Taglialatela-Scafati, O. Antimalarials based on the dioxane scaffold of plakortin. A concise synthesis and SAR studies. *Bioorg. Med. Chem.* **2011**, *19*, 312–320.
(18) MMV: Medicines for Malaria Venture. http://www.mmv.org.
(19) Dembitsky, V. M. Bioactive peroxides as potential therapeutic agents. *Eur. J. Med. Chem.* **2008**, *43*, 223–251.
(20) Tang, Y.; Dong, Y.; Vennerstrom, J. L. Synthetic peroxides as antimalarials. *Med. Res. Rev.* **2004**, *24*, 425–448.
(21) Vennerstrom, J. L.; Arbe-Barnes, S.; Brun, R.; Charman, S. A.; Chiu, F. C. K.; Chollet, J.; Dong, Y.; Dorn, A.; Hunziker, D.; Matile, H.; McIntosh, K.; Padmanilayam, M.; Santo Tomas, J.; Scheurer, C.; Scorneaux, B.; Tang, Y.; Urwyler, H.; Wittlin, S.; Charman, W. N. Identification of an antimalarial synthetic trioxolane drug development candidate. *Nature* **2004**, *430*, 900–904.
(22) Singh, C.; Hassam, M.; Naikade, N. K.; Verma, V. P.; Singh, A. S.; Puri, S. K. Synthesis and antimalarial assessment of a new series of orally active amino-functionalized spiro 1,2,4-trioxanes. *J. Med. Chem.* **2010**, *53*, 7587–7598.
(23) Bousejra-El Garah, F.; Claparols, C.; Benoit-Vical, F.; Meunier, B.; Robert, A. The antimalarial trioxaquine DU1301 alkylates heme in malaria-infected mice. *Antimicrob. Agents Chemother.* **2008**, *52*, 2966–2969.
(24) O'Neill, P. M.; Amewu, R. K.; Nixon, G. L.; Bousejra ElGarah, F.; Mungthin, M.; Chadwick, J.; Shone, A. E.; Vivas, L.; Lander, H.; Barton, V.; Muangnoicharoen, S.; Bray, P. G.; Davies, J.; Park, B. K.; Wittlin, S.; Brun, R.; Preschel, M.; Zhang, K.; Ward, S. A. Identification of a 1,2,4,5-tetraoxane antimalarial drug-development candidate (RKA 182) with superior properties to the semisynthetic artemisinins. *Angew. Chem., Int. Ed.* **2010**, *49*, 5693–5697.
(25) Dong, Y.; McCullough, K. J.; Wittlin, S.; Chollet, J.; Vennerstrom, J. L. The structure and antimalarial activity of dispiro-1,2,4,5-tetraoxanes derived from (+)-dihydrocarvone. *Bioorg. Med. Chem. Lett.* **2010**, *20*, 6359–6361.
(26) Muraleedharan, K. M.; Mitchell, A. A. Progress in the development of peroxide-based anti-parasitic agents. *Drug Discovery Today* **2009**, *14*, 793–803.
(27) Watts, K. R.; Tenney, K.; Crews, P. The structural diversity and promise of antiparasitic marine invertebrate-derived small molecules. *Curr. Opin. Biotechnol.* **2010**, *21*, 808–818.
(28) Fattorusso, E.; Taglialatela-Scafati, O. Marine antimalarials. *Mar. Drugs* **2009**, *7*, 130–152.
(29) Tategami, S.; Yamada, T.; Nishino, H.; Korp, J. D.; Kurosawa, K. Formation of 1,2-dioxacyclohexanes by the reaction of alkenes with tris(2,4-pentanedionato)manganese(III) or with β-ketocarbonyl compounds in the presence of manganese(III) acetate. *Tetrahedron Lett.* **1990**, *31*, 6371–6374.
(30) Yoshida, J.; Nakatani, S.; Sakaguchi, K.; Isoe, S. Formal [2 + 2 + 2] cycloaddition of molecular oxygen, 1,3-diketone, and olefin. Synthesis and reactions of cyclic peroxides. *J. Org. Chem.* **1989**, *54*, 3383–3389.
(31) Nishino, H. Manganese(III)-based peroxidation of alkenes to heterocycles. *Top. Heterocycl. Chem.* **2006**, *6*, 39–76.
(32) (a) Snider, B. B. Manganese(III)-based oxidative free-radical cyclizations. *Chem. Rev.* **1996**, *96*, 339–363. (b) Linker, T. Selective reactions of transition-metal-generated radicals. *J. Organomet. Chem.* **2002**, *661*, 159–167.
(33) Posner, G. H.; O'Dowd, H.; Ploypradith, P.; Cumming, J. N.; Xie, S.; Shapiro, T. A. Antimalarial cyclic peroxy ketals. *J. Med. Chem.* **1998**, *41*, 2164–2167.
(34) Donkers, R. L.; Workentin, M. S. Elucidation of the electron transfer reduction mechanism of anthracene endoperoxides. *J. Am. Chem. Soc.* **2004**, *126*, 1688–1698.
(35) (a) Arantes, C.; de Araujo, M. T.; Taranto, A. G.; Carneiro, J. W. D. Relative stability of radicals derived from artemisinin: a semiempirical and DFT study. *Int. J. Quantum Chem.* **2005**, *103*, 749–762. (b) Drew, M. G. B.; Metcalfe, J.; Dascombe, M. J.; Ismail, F. M. D. De novo identification and stability of the artemisinin pharmacophore: studies of the reductive decomposition of deoxyartemisinins and deoxyarteethers and the implications for the mode of antimalarial action. *J. Mol. Struct.: THEOCHEM* **2007**, *823*, 34–46.
(36) (a) Posner, G. H.; Wang, D.; Cumming, J. N.; Oh, C. H.; French, A. N.; Bodley, A. L.; Shapiro, T. A. Further evidence supporting the importance of and the restrictions on a carbon-centered radical for high antimalarial activity of 1,2,4-trioxanes like artemisinin. *J. Med. Chem.* **1995**, *38*, 2273–2275. (b) Robert, A.; Benoit-Vical, F.; Dechy-Cabaret, O.; Meunier, B. From classical antimalarial drugs to new compounds based on the mechanism of action of artemisinin. *Pure Appl. Chem.* **2001**, *73*, 1173–1188.
(37) Kawanishi, M.; Kotoku, N.; Itagaki, S.; Horii, T.; Kobayashi, M. Structure–activity relationship of anti-malarial spongean peroxides having a 3-methoxy-1,2-dioxane structure. *Bioorg. Med. Chem.* **2004**, *12*, 5297–5307.
(38) Posner, G. H.; Oh, C. H.; Wang, D.; Gerena, L.; Milhous, W. K.; Meshnick, S. R.; Asawamahasadka, W. Mechanism-based design, synthesis, and in vitro antimalarial testing of new 4-methylated trioxanes structurally related to artemisinin: the importance of a carbon-centered radical for antimalarial activity. *J. Med. Chem.* **1994**, *37*, 1256–1258.
(39) Jefford, C. W. Why artemisinin and certain synthetic peroxides are potent antimalarials. Implications for the mode of action. *Curr. Med. Chem.* **2001**, *8*, 1803–1826.
(40) (a) Galasso, V.; Kovač, B.; Modellic, A. Theoretical and experimental study on the molecular and electronic structures of artemisinin and related drug molecules. *Chem. Phys.* **2007**, *335*, 141–154. (b) Gu, J.; Chen, K.; Jiang, H.; Ji, R. DFT study of artemisinin and 1,2,4-trioxane. *J. Mol. Struct.: THEOCHEM* **1999**, *459*, 103–111. (c) Thomson, C.; Cory, M.; Zerner, M. Theoretical studies of some new anti-malarial drugs. *Int. J. Quantum Chem.* **1991**, *40*, 231–245.
(41) Haynes, R. K.; Vonwiller, S. C. The behaviour of qinghaosu (artemisinin) in the presence of non-heme iron(II) and (III). *Tetrahedron Lett.* **1996**, *37*, 257–260.
(42) Avery, M. A.; Gao, F. L.; Chong, W. K. M.; Hendrickson, T. F.; Inman, W. D.; Crews, P. Synthesis, conformational analysis, and antimalarial activity of tricyclic analogs of artemisinin. *Tetrahedron* **1994**, *50*, 957–972.
(43) Maple, J. R.; Hwang, M. J.; Stockfisch, T. P.; Dinur, U.; Waldman, M.; Ewig, C. S.; Hagler, A. T. Derivation of class II force fields. I. Methodology and quantum force field for the alkyl function group and alkane molecules. *J. Comput. Chem.* **1994**, *15*, 162–182.
(44) Fletcher, R. Unconstrained Optimization. In *Practical Methods of Optimization*; John Wiley & Sons: New York, 1980; Vol. *1*.
(45) Stewart, J. J. P. Optimization of parameters for semiempirical methods V: modification of NDDO approximations and application to 70 elements. *J. Mol. Model.* **2007**, *13*, 1173–1213.
(46) *MOPAC2009*; Stewart Computational Chemistry: Colorado Springs, CO, 2008; http://OpenMOPAC.net.
(47) Baker, J. An algorithm for the location of transition states. *J. Comput. Chem.* **1986**, *7*, 385–395.
(48) Holtje, H. D.; Fattorusso, C. Construction of a model of the *Candida albicans* lanosterol 14-alpha-demethylase active site using the homology modelling technique. *Pharm. Acta Helv.* **1998**, *72*, 271–277.

(49) Ding, H. Q.; Karasawa, N.; Goddard, W. A. III. Atomic level simulations on a million particles: the cell multipole method for Coulomb and London non-bond interactions. *J. Chem. Phys.* **1992**, *97*, 4309−4315.
(50) Frisch, M. J.; Trucks, G. W.; Schlegel, H. B.; Scuseria, G. E.; Robb, M. A.; Cheeseman, J. R.; Scalmani, G.; Barone, V.; Mennucci, B.; Petersson, G. A.; Nakatsuji, H.; Caricato, M.; Li, X.; Hratchian, H. P.; Izmaylov, A. F.; Bloino, J.; Zheng, G.; Sonnenberg, J. L.; Hada, M.; Ehara, M.; Toyota, K.; Fukuda, R.; Hasegawa, J.; Ishida, M.; Nakajima, T.; Honda, Y.; Kitao, O.; Nakai, H.; Vreven, T.; Montgomery, J. A., Jr.; Peralta, J. E.; Ogliaro, F.; Bearpark, M.; Heyd, J. J.; Brothers, E.; Kudin, K. N.; Staroverov, V. N.; Kobayashi, R.; Normand, J.; Raghavachari, K.; Rendell, A.; Burant, J. C.; Iyengar, S. S.; Tomasi, J.; Cossi, M.; Rega, N.; Millam, N. J.; Klene, M.; Knox, J. E.; Cross, J. B.; Bakken, V.; Adamo, C.; Jaramillo, J.; Gomperts, R.; Stratmann, R. E.; Yazyev, O.; Austin, A. J.; Cammi, R.; Pomelli, C.; Ochterski, J. W.; Martin, R. L.; Morokuma, K.; Zakrzewski, V. G.; Voth, G. A.; Salvador, P.; Dannenberg, J. J.; Dapprich, S.; Daniels, A. D.; Farkas, Ö.; Foresman, J. B.; Ortiz, J. V.; Cioslowski, J.; Fox, D. J. *Gaussian 09*, revision A.1; Gaussian, Inc.: Wallingford, CT, 2009.
(51) Allouche, A. R. A graphical user interface for computational chemistry softwares. *J. Comput. Chem.* **2011**, *32*, 174−182.
(52) Becke, A. D. Density-functional thermochemistry. III. The role of exact exchange. *J. Chem. Phys.* **1993**, *98*, 5648−5652.
(53) Lee, C.; Yang, W.; Parr, R. G. Development of the Colle−Salvetti correlation-energy formula into a functional of the electron density. *Phys. Rev.* **1988**, *B37*, 785−789.
(54) Frisch, M. J.; Pople, J. A.; Binkley, J. S. Self-consistent molecular orbital methods. 25. Supplementary functions for Gaussian basis sets. *J. Chem. Phys.* **1984**, *80*, 3265−3269.
(55) Chiodo, S.; Russo, N.; Sicilia, E. Newly developed basis sets for density functional calculations. *J. Comput. Chem.* **2004**, *26*, 175−183.
(56) Liu, Y.-P. Applications of effective core potentials and density functional theory to the spin states of iron porphyrin. *J. Chem. Inf. Comput. Sci.* **2001**, *41*, 22−29.
(57) Ruiz, E.; Cirera, J.; Alvarez, S. Spin density distribution in transition metal complexes. *Coord. Chem. Rev.* **2005**, *249*, 2469−2660.
(58) (a) Peng, C; Schlegel, H. B. Combining synchronous transit and quasi-Newton methods to find transition states. *Isr. J. Chem.* **1993**, *33*, 449−454. (b) Peng, C.; Ayala, P. Y.; Schlegel, H. B.; Frisch, M. J. Using redundant internal coordinates to optimize equilibrium geometries and transition states. *J. Comput. Chem.* **1996**, *17*, 49−56.
(59) (a) Gonzalez, C.; Schlegel, H. B. An improved algorithm for reaction path following. *J. Chem. Phys.* **1989**, *90*, 2154−2161. (b) Gonzalez, C.; Schlegel, H. B. Reaction path following in mass-weighted internal coordinates. *J. Phys. Chem.* **1990**, *94*, 5523−5527.
(60) Trager, W.; Jensen, J. B. Human malaria parasites in continuous culture. *Science* **1976**, *193*, 673−675.
(61) (a) Makler, M.; Hinrichs, D. Measurement of the lactate dehydrogenase activity of *Plasmodium falciparum* as an assessment of parasitemia. *Am. J. Trop. Med. Hyg.* **1993**, *48*, 205−210. (b) Sparatore, A.; Basilico, N.; Parapini, S.; Romeo, S.; Novelli, F.; Sparatore, F.; Taramelli, D. 4-Aminoquinoline quinolizidinyl- and quinolizidinylalkyl-derivatives with antimalarial activity. *Bioorg. Med. Chem.* **2005**, *13*, 5338−5345.
(62) Ades, E. W.; Candal, F. J.; Swerlick, R. A.; George, V. G.; Summers, S.; Bosse, D. C.; Lawley, T. J. HMEC-1: establishment of an immortalized human microvascular endothelial cell line. *J. Invest. Dermatol.* **1992**, *99*, 683−690.
(63) D'Alessandro, S.; Gelati, M.; Basilico, N.; Parati, E. A.; Haynes, R. K.; Taramelli, D. Differential effects on angiogenesis of two antimalarial compounds, dihydroartemisinin and artemisone: implications for embryotoxicity. *Toxicology* **2007**, *241*, 66−74.